*We thank all reviewers for helpful comments and suggestions. All comments are addressed below in a point-by-point response, indicated in italics.*

**Reviewer 1:**

General Comments: This paper provides a nice overview of the CAM4-chem simulations that have been performed for CCMI. It describes the model configurations used, simulations conducted, and updates made to the model. Preliminary analyses of the model results relative to observations are also shown.

Detailed documentation of model simulations that will likely be used in a wide range of analyses through the CCMI effort is extremely useful. Someone wishing to use the model output from these simulations, but is otherwise unfamiliar with the details concerning this model, will find this write-up to be a great reference when trying to understand how the CAM4-chem model differs from the other models participating in CCMI. All information included in this manuscript is relevant and complete for under- standing the details of this model simulation, and the preliminary analysis of the results compared to observations is instructive. I therefore recommend the publication of this manuscript with minor revisions.

Specific Comments: The motivations for some of the specific changes to the model are unclear; a brief statement of why deviations from the previous version of the model or from a method described in the literature would be helpful. Instances where I'd like to see a bit more explanation include:

Page 2, Line 28 (Section 2.1): A brief mention of what issue is addressed by the improvements to the deep convection scheme (Richter and Rasch, 2008; Neale et al., 2008) would be instructive to a reader who is not so familiar with dynamics.

*We agree with the reviewer and give some more detailed information in the text:* ***"In summary, deep convection is treated by Zhang et al. (1995) with improvements in the convective momentum transport (Richter et al., 2008), which improved surface winds, stresses, and tropical convection. At the same time, an entraining plume was added to the convection parameterization, which together with the momentum transport improved the representation of t*****he El Nino–Southern Oscillation (ENSO)*** ***significantly (Neale et al., 2008)."***

Page 5, Line 7 (Section 2.1.6): Is there a reason for using Leaf Area Index "from the previous model timestep instead of the average of the previous 10 days"? Is there any significant difference between biogenic emissions calculated this way versus calculated by the method of Guenther et al. (2012)?

*Guenther et al (2012) used monthly mean LAI maps, so in that case, the 'previous timestep' meant the average of the previous month. In the original implementation of MEGANv2.1 in CLM, this was erroneously interpreted as the previous model timestep (30 min). To be consistent with other formulas in the MEGAN algorithm (and in consultation with Alex Guenther), we corrected the CLM implementation to use LAI averaged over the previous 10 days. A corrected implementation is closer to the algorithm of Guenther et al. (2012).*
We changed the text to:

***"An erroneous implementation of MEGAN in this version differs from the description of Guenther et al. (2012) by using the LAI from the previous model timestep (30 minutes) instead of the average of the previous 10 days. In addition, in this version we are using a fixed $CO_2$ mixing ratio, instead of the simulated atmospheric value, in the calculation of the $CO_2$ inhibition effect on isoprene emissions. The corrected implementation is closer to the algorithm of Guenther et al. (2012)."***

Other Specific Comments: Page 5, Line 14 (Section 2.2): The synthetic tracers that are recommended by CCMI and included in these simulations are listed, then the O3S tracer is described. I understand that the reader could refer to the SPARC newsletter for a description of the remaining tracers, but it would be instructive to have those descriptions in this paper as well. They do not need to be defined individually, necessarily; a categorization or brief description of the usefulness of the tracers is sufficient.

*We mention O3S here, because it may have been treated differently than in other models due to the interpretation of the recommendation in Eyring et al. (2013) for this tracer. We have interpreted the recommendation by CCMI to not include dry deposition for this tracer, which has to be pointed out in the text. For the other tracers, a good description is indeed given in Eyring et al., 2013. To make it easier for the reader, we give the Section number in Eyring et al., 2013, so one has an easier time finding the description.*

Page 7, Line 25 (Section 3.1): "Differences in clouds and land surface temperatures" cause the differing VOC emissions between simulations. Prior to this, it is pointed out that REFC1SD had higher land temperatures; shouldn't higher temperatures generally lead to greater emissions of biogenic VOCs though? Does this mean clouds are causing an even larger difference in emissions rates, if the effect of temperature is compensating? An explicit statement of why you think VOC emission rates in the SD run are so much lower than in the FR runs would be beneficial here.

*Without performing additional sensitivity study we can only speculate on the reason for differences between the two simulations. However, there are indications that differences in clouds play an important role. There are more low clouds in the SD simulation, as the short-*

*wave cloud forcing is a bit higher (about 30%) than the FR simulations and j-values are reduced near the surface.*

*"Differences in clouds and land surface temperatures between the reference experiments result in different biogenic emissions of volatile organic components (VOCs) (Figure~\ref{fi emis_bio}). REFC1SD biogenic emissions are about 10\% lower than in the REFC1 experiment and about 15\% lower than in the REFC2 experiment. The emissions differ the most in summer during their peak (Figure 1, bottom row).* ***Despite the fact that surface temperatures in REFC1SD are warmer than in REFC1, more low cloud clouds and reduced solar radiation (as evident in photolysis rates) near the surface may be the important driver for the reduced biogenic emissions in REFC1SD, which has to be further investigated.****"*

Page 8, Line 16 (Section 3.2): A link between increasing methane emissions and increases in tropospheric OH is suggested here. However, the general view is that OH should decrease with increasing burdens of methane, since methane is a sink for OH. Perhaps this could be clarified.

*This was a typo in the manuscript, methane emissions are decreasing between 1980 and 2010 and this corresponds to the increase in tropospheric OH. We fixed the text accordingly.*

Page 8, Line 23 (Section 3.2): "larger ozone mixing ratios in the upper troposphere in the REFC1SD experiment results in a higher oxidation capacity", however, primary production of OH in the upper troposphere is often limited by concentrations of water vapor, and so the UT has little influence on the oxidative capacity of the troposphere. Is there clear evidence in support of this conclusion? It would be helpful to state or show what led to this statement.

*We agree that the statement was not sufficiently supported. Other reasons for differences in methane lifetime could be changes in photolysis due to changes in high clouds. We have changed the sentence:*

*"For instance, larger ozone mixing ratios in the upper troposphere in the REFC1SD experiment results in a higher oxidation capacity of the troposphere and therefore a shorter lifetime of methane compared to the other experiments."*

To

***"The shorter lifetime of methane in REFC1SD compared to the other experiments may be a result of a reduction in high clouds, and, to a small extent, larger ozone mixing ratios in the tropical troposphere, which would increase the oxidation capacity in the tropics. This has to be investigated in more detail in future studies."***

Page 10, Line 12 (Section 4.1.1): Why is the model overestimating winter ozone mixing ratios in

the UT? STE?

*Transport problems in the model may be the reason for the overestimation. In a follow-on study, it turns out that the nudging amount of 1% is impacting the convection in REFC1SD in a non optimal way in the troposphere (Jessica Neu, personal communication). A nudging value of 10% is improving ozone values in the UTLS. To add this information, we change the sentence to:*

*"At 250 hPa, which is in the UTLS at mid and high latitudes, REFC1SD overestimates ozone by up to 50%, particularly at mid latitudes in both hemispheres.* ***This could be the result of strong mixing in the UTLS associated with the use of the small nudging amount of 1% in this study; however this needs to be investigated in more detail in future studies.*** *The other experiments show smaller deviations from the observations of about 20% or less."*

Figure 1: Labels that define the colors, as in Figure 2, would be helpful here.

*These have been added.*

Technical Corrections: Page 1, Line 7 (Abstract): "observed period" is unclear; perhaps "satellite era" instead?

*We change this to: "We summarize the performance of the three reference simulations suggested by CCMI,* ***with a focus on the last 15 years of the simulation when most observations are available****."*

Page 1, Line 13 (Abstract): "has been" should be "is"

*changed*

Page 2, Line 31 (Section 2.1): semi-colon between references should be an "and"

*changed*

Page 3, Line 9 (Section 2.1.1): Meaning of "above 100 hPa" could be confused; suggest "at pressures less than 100 hPa" or something similar to make it absolutely clear

*changed*

Page 4, Line 23 (Section 2.1.4): "black carbon and primary organic carbon, nitrates are..." should be "black carbon, primary organic carbon, and nitrates are..."

*changed*

Page 5, Line 2 (Section 2.1.6): acronym used is "CLM" but was introduced as "CLM4.0"

*changed*

Page 5, Line 30 (Section 2.2): Second “C” in “CAM4-Chem” should be lower case for consistency

*changed*

Page 6, Line 3 (Section 2.2): semi-colon between references should be “and” Page 6, Line 10 (Section 2.2): The “1” in “O1D” should be superscripted

*changed*

Page 7, Line 5 (Section 2.3.1): Should “ran until 1959” be “ran through 1959”? The meaning conveyed is slightly different.

*Changed, “through” is correct*

Page 8, Line 2 (Section 3.1): Methane lifetime due to OH reported in Supplement of Prather et al. is 11.2 years, not 11.3

*changed*

Page 8, Line 7 (Section 3.1): “optical depth is with around 0.04 somewhat higher than...” should be “optical depth around 0.04 is somewhat higher than...”

*changed*

Page 8, Line 15 (Section 3.2): Specify “increasing column ozone” as “increasing tropospheric column ozone”

*changed*

Page 8, Line 26 (Section 3.2): Would like to see a reference here; there are plenty of candidate papers.

*We added “WMO2006”*

Page 9, Line 14 (Section 4.1.1): “altitudes below 900 hPa can be confusing to mix altitude and pressure coordinates; same just below in Line 16

*This has been fixed.*

Page 9, Line 15 (Section 4.1.1): Definition of MOZAIC acronym is not correct, compared to

website

*Thanks for pointing that out, the acronym is now: "**Measurements of OZone, water vapour, carbon monoxide and nitrogen oxides by in-service AIrbus airCraft**"*

Page 10, Line 9 (Section 4.1.1): Punctuation in "U.S. . REFC1/REFC2" should be fixed

*changed*

Page 10, Line 30 (Section 4.1.2): "The ozone gradient... is to the most part well captured" should be "...is for the most part well captured".

*changed*

Page 11, Line 25 (Section 4.2): "the model underestimate" should be "the model underestimates"

*changed*

Page 12, Line 17 (Section 4.4): "over the remote region over the Pacific" should be

"over the remote region of the Pacific"

*changed*

Page 13, Line 5 (Section 5): "investiaged" should be "investigated"

*changed*

Page 13, Line 18 (Section 5): remove "rather"

*changed*

Figure 5, Caption: time period (1995-2011) is not consistent with time period in the text (Pg. 10, Line 14: 1995-2010)

*The ozonesonde climatology is derived for the period between 1995-2011, while the model results for this comparison are between 1995-2010. We clarified this in the text and the figure caption.*

***"A comparison with ozonesonde observations over different regions for simulated years between 1995-2010 …"***

Table A1, Title: "semi-implicit (S)" should be "semi-implicit (I)"

*changed*

**Reviewer 2:**

Summary: This is a technical paper that summarizes the make-up and performance of the CAM4-chem model for the CCMI simulations. Publication of a paper like this is highly desirable for the CCMI models as it greatly aids the interpretation of these simulations. The paper is well-written. My major comments listed below relate to the model more than the paper; they amount to a minor revision of the paper.

At 40 km, CAM4-chem has an exceptionally low upper lid. There is some evidence in the literature that such a low lid influences stratospheric dynamics and consequently chemistry (although related factors such as differences in model physics between high- and low-top models may also influence this). By comparing CAM4-chem with the high- top version of CESM1, WACCM, it may well be possible to tease out these influences. A comprehensive discussion of how this is reflected in the CAM4-chem behaviour would be interesting but is beyond the scope of this paper.

*We agree that this discussion is beyond the scope of this paper and a future paper will address this question. However, we have compared the CAM4-chem results with WACCM results in the troposphere, and there is very little difference. So, for tropospheric chemistry, the low-top model is behaving very similarly to the high top model.*

The authors note that there are some significant differences in model behaviour between the specified-dynamics and the free-running model. This will be of interest to an ongoing model evaluation activity which focusses on the specified-dynamics runs.

*We agree with the reviewer. Such an activity has started after the October 2015 CCMI Workshop and is led by Clara Orbe (NASA)*

Substantial differences w.r.t. observations are found for the simulation of hydrocarbons. This could be related to the treatment of emissions, i.e. the distribution of generic "NMVOC" emissions across the primary source gases represented in the model. How is this handled here? Do you use any lumping?

*It is certainly possible that errors are introduced in the speciation of total NMVOC to the individual model species. Emissions were provided for CCMI in a standard VOC speciation (described in Section 2.3). In the comparisons we have made to observations, hydrocarbons are all generally under-estimated, indicating the overall emissions are too low, and that it is not purely a problem with the speciation. The chemical species included in CAM4-chem are listed in Table A1. The hydrocarbons ethane, ethene, ethyne, propane, propene, benzene, toluene and xylenes are treated explicitly, while BIGALK and BIGENE represent lumped alkanes and alkenes,*

*respectively, for C>3. Several VOCs are treated explicitly (CH2O, CH3CHO, CH3COCH3, CH3OH, C2H5OH), but some are lumped (e.g., MEK).*

Detailed comments:

P3L9: Replace "terrain-following" with "hybrid terrain-following pressure"

*changed*

P3L11: This difference in vertical resolution is perhaps a little disappointing as it introduces differences into the experiments that are not directly due to the specified dynamics versus free-running experiments.

*We agree that introducing a different vertical resolution without any nudging of met fields would likely change the performance of the model a bit. Past experience with changing the vertical resolution of the analysis data (to match the free-running grid) showed very significant deterioration in the quality of the simulation.*

P3L12: Exactly which fields are being nudged? Do "meteorological fields" include moisture variables? How about differences in orography between the reanalysis grid and the model, which can introduce imbalances into the model? This may not be an issue if MERRA uses the same grid and orography as CAM4-chem.

*For the SD configuration, internally derived meteorological fields, including wind components, temperature, surface pressure, surface stress, and latent and sensible heat flux are nudged to MERRA. The MERRA reanalysis fields are interpolated to the horizontal resolution of the model prior to running the simulation. The MERRA surface geopotential height is used for the SD simulations to be consistent with the reanalysis fields.*

*We adjust the text accordingly:*

*"**Nudged meteorological fields include zonal wind components, temperatures, surface pressure, surface stress, latent, and sensible heat flux. Analyzed fields are interpolated to the horizontal resolution of the model. The MERRA surface geopotential height is used for the SD simulations to be consistent with the reanalysis fields.**"*

P4L7ff: Does this error in the formulation of IGW mean that the model gets it right for the wrong reason? Do you have any experience with a version of the model that is not affected by this problem? The improved behaviour despite the above error suggests that either the above

is true, or this process may not be important after all. Also this seems to be a new process which affects gyroscopic pumping. Do you need to change the other forms of GWD accordingly, to keep the Brewer-Dobson circulation intact?

*The comparison of our simulations with those of Garcia et al (2016) and many other simulations (for testing) shows that it is important to have gravity wave drag from waves that have both relatively high momentum flux magnitudes and low horizontal phase speeds; beyond this, the details of how these waves are specified do not have much impact on the simulations as stated in the text. What seems to matter most is that the amplitude and timing of the gravity wave drag.*

P5L16ff: I suspect this is a misinterpretation of the formulation used by Eyring et al., SPARC Newsletter (2013). $O_3S$ is defined as identical to $O_3$ in the stratosphere but only subject to loss but not production in the troposphere. That loss must include dry deposition otherwise the straightforward interpretation of $O_3S$ as constituting the stratospheric contribution to $O_3$ is no longer possible. The word "ozone *chemical* loss rate" used by Eyring et al. (2013) is unfortunate in this regard. Other CCMI modellers will have interpreted this differently. Also aside from the dry deposition issue, what constitutes the correct "chemical loss rate" to apply in this context is subject to an on-going debate. Which rate do you apply?

*We agree that the wording was confusing and could also be interpreted differently. To address the comment, we change "Following the CCMI recommendation, " to "**As interpreted from the CCMI recommendation**". Regarding the chemical loss rate, we apply the definition listed on Page 6, Line 9.*

P6L20: Is that "HadISST2"? Please specify the version. P8L7: "At 0.04, the dust optical depth is somewhat larger than. . ." P8L14ff: This sentence is too convoluted to understand. Please rephrase / clarify.

*Changed*

P10L14f: Are you sure that "all model experiments reproduce observed tropospheric ozone within 20%"? This is a very far-reaching statement. I'd phrase this more carefully.

*We change the sentence to:*

*"**Besides some differences in ozone compared to observations, as discussed above, all model experiments reproduce observed tropospheric ozone within 25% for most of the regions**."*

P11L25: "underestimates"

*changed*

P12L5: “by up to 5 times in spring”: I suggest to replace this phrase by “The model underestimates ethane by up to 80%.”

*changed*

P13L13: “the mid-latitude UTLS” P13L17: replace “ascribed” with “attributed” P13L19: replace “great” with “large an” P16L24: "McFarlane"

*changed*

**Reviewer 3:**

Review of: “Representation of the Community Earth System Model (CESM1) CAM4- chem within the Chemistry-Climate Model Initiative (CCMI)” by Tilmes et al.

This paper documents the configuration of CAM4-chem used in the CCMI simulations. It documents updates to CAM4-chem and compares CAM4-chem simulations to measurements in three simulation configurations. It is particularly nice that the paper documents some of the successes of CAM4-chem as well as aspects of the simulations that do not agree with measurements. In and of itself the paper offers model refinements, but does not seem to offer any particularly new model developments or new science not documented elsewhere. The interest of this paper is that it acts as a background for further analysis of the CCMI model runs and thus will be useful to the community at large in subsequent analysis. It will be particularly useful if other modeling groups post similar papers (hopefully using similar diagnostics). I would recommend publication following minor revisions.

A few general aspects of this paper could be improved (see specific comments below). (i) Some more detail concerning differences in the model simulations should be included. (ii) In a few places the results would benefit from additional analysis. (iii) Some aspects of the paper organization detailing the simulations and model could be improved. (iv) A number of figures are put into the appendix. It is not really obvious why this is done. It just makes it harder for the reader to refer to these figures. The figures in the appendix seem as relevant as those in the main body of the paper. I would suggest including them in the main body of the text.

i) *We agree with the reviewer to include more detailed information regarding the model simulations, see comments below.*
ii) *The scope of the paper is to document the specific model configurations for CCMI and new developments of the model. We highlight some agreements and*

*disagreements of the model with observations. Additional analyses will be performed in future studies and multi-model analysis.*

iii) *Regarding figures in the Appendix, we tried to make the paper more concise in not including all the figures in the main paper that do not contribute to new findings. However, we would like to add them for the reader as backup information. We address the specific figures mentioned by the reviewer below.*

Comments:

1. It would be useful right in the first paragraph to specify the simulation periods for each of the CCMI simulations (REFC1, REFC1SD and REFC2).

*This information has been added.*

2. P2,L12: "reference CCMI model experiments". It would be worthwhile to emphasize that this is using CAM4-chem in particular – the summarization is not for CCMI models in *general.*

*We added CESM1 CAM4-chem*

3. The introduction does not explicitly mention model-measurement evaluation. It seems that it is important to explicitly mention this as a focus of the paper. It may be worthwhile to point out from the beginning that this paper forms the basis for a more in-depth analysis.

*The text already mentions the model-measurement evaluation:*

*".. and evaluate selected diagnostics based on observational data sets in Section 4. We employ existing and new datasets to evaluate the general performance of the model."*

*To address the comment, we add:*

*"More in-depth analysis and evaluations will follow in multi-model comparison studies."*

4. P2,L22, "The land model". It would be worthwhile stating that the version of the land model used here does not include interactive carbon and nitrogen cycling.

*The version of the land model can be run with interactive carbon and nitrogen cycle, however, in our configuration, this was not included.*

*We change "The land model does not include an interactive carbon or nitrogen cycle and only the atmospheric and land components are coupled to the chemistry."*

*To*

*"The land model was **run without** an interactive carbon or nitrogen cycle and only the atmospheric and land components are coupled to the chemistry."*

5. P2,L28 and P3,L25: "McFarlanle"

*corrected*

6. Section 2.1. Please state explicitly whether aerosols impact model photolysis.

*We added the following:*

*"**Only changes in the ozone column, but not in the aerosol burden, impact photolysis rates.**"*

7. Section 2.1.1. The vertical grid is in hybrid coordinates, transitioning from pure sigma near the surface to pressure in the stratosphere.

*We changed the text:*

***"The vertical coordinate is sigma hybrid terrain-following pressure in the troposphere, switching over to isobaric at pressure levels less than 100 hPa;"***

8. P3, L13. Please state which fields are nudged and the time resolution of the input meteorological fields.

*We added to the text:*

"***Nudged meteorological fields include wind components, temperatures, surface pressure, surface stress, latent, and sensible heat flux. Analyzed fields are interpolated to the horizontal resolution of the model. The MERRA surface geopotential height is used for the SD simulations to be consistent with the reanalysis fields."***

9. The QBO (2.1.2). It would be interesting to know if nudging to the QBO impacts the tropospheric chemistry simulation.

*This is an interesting question, which however cannot be addressed in this paper.*

10. P5,L8. "simulated atmospheric value". It is unclear to me to what extent atmospheric CO2 is simulated: is it simulated or specified? Also, does ozone feedback onto the atmospheric radiation budget?

*We add a clarification on emissions, lower boundary conditions, and radiatively active species in this section*:

*"**Emissions of gas-phase and aerosol species, as indicated in Table A1, are in general distributed at the surface. Only aircraft emissions of BC and nitrogen dioxide, and volcanic emissions of sulfur and sulfate, are vertically distributed. Species with lower boundary conditions, listed in Table A1, as discussed in Section 2.3.2."***

*and later on*

*"**All aerosols and some gas-phase species, including H2O, O2, CO2, O3, N2O, CH4, CFC11, CFC12, are radiatively active**."*

11. P5, L14. It doesn't make sense to me to list all these tracers in the text. Most readers will have no idea what they are. Listing in the table should suffice.

*We list the tracers to indicate which ones have been included. We also add a detailed reference, Eyring et al., 2013,* Section 4.2.1, *to make it easy for the reader to look up the meaning of the tracers.*

12. P6, L3. The description of lightning NOx does not really belong in the section characterizing the chemical mechanism.

*We agree and move it to the atmosphere model section.*

13. Section 2.2 . There really is hardly any aerosol description in this section (aerosols are described in 2.1.4 and 2.1.5). Some reorganization here would make sense.

*We agree with the reviewer and rename section 2.2 to: "Chemical mechanism" and move the one sentence on aerosols to Section 2.1.5.*

14. Section 2.3. Personally, I would put this section above to give the reader some idea of the simulations before going into details about the model. Much of the information on nudging here seems a repeat (but in more detail) of information above.

*The experimental setup of the model is independent of the model description. Other experiments, for example HTAP, would use the same model code. Therefore, we think it makes more sense to keep it separated*.

Please include years of the simulations here (they are included under initial conditions and spinup below). It would be helpful if you could summarize the emission differences between the simulations and possibly put some of the 1995-2010 emission totals in Table 1. The emission differences between the simulations are important for interpreting the results. The emissions for C1SD and C1 are exactly the same, correct? This should be explicitly stated.

Emissions in C1 and C1SD show much higher interannual variability than C2 (figure A1). Is this due to biomass burning emissions or something else? The reasons for this should be stated explicitly. Are there mean emission differences between C2 and C1: if so please state what these are.

*The emissions for the different experiments are shown in Figure A1. The time evolution and differences in variability are more obvious if shown in a figure than giving total numbers. We adjust the text to clarify differences between the emissions.*

*"**The three reference experiments are performed with the recommended emissions. REFC1 and REFC1SD (years 1960-2010), use the same emissions, excluding biogenic emissions. Anthropogenic and biomass burning emissions are from the MACCity emission data set and change every year Granier et al. (2011). For REFC2 (years 1960-2100), anthropogenic and biomass burning emissions are taken from AR5 (Eyring et al., 2013) (see Figure A1), which only vary every 5-10 years. All emissions include a seasonal cycle. All biogenic emissions are calculated every timestep by MEGAN, as described in Section 2.1.6.**"*

Are the differences between REFC1 and REFC2 over the historical period only due to differences in the emissions, or can differences be attributed to something else in addition? In summary some additional clarity in the differences between these simulations would be valuable.

*As can be seen from Figure A1 differences in emissions will have some impact. However, since REFC2 is couple to the ocean, the climate will also be different, which has of course a large impact on the atmospheric composition.*

15. P7, L24, Can you quote measurement estimates of SWCF? Is the REFC1SD outside the measured range?

*Observed global numbers of SWCF are between 47 W/m2 (CERES) and 54 W/m2 (ERBE). We adjusted the text:*
*"**In the REFC1SD experiment, low cloud fraction is significantly larger than in the other experiments, which results in a much smaller shortwave cloud forcing (SWCF) of -83 W/m2 compared the other experiments that are with 54-56 W/m2 more in line with observations**."*

16. P7, Figure 1. It would be helpful to know the extent that the emissions given in Figure 1 are internally calculated. Section 2.1.6 does not specify which biogenic emissions are calculated. To what extent are the emission differences in the VOCs due to those in the biogenic emissions? Do differences in biogenic emissions account for all the differences between the C1SD and C1 VOC emissions? To what extent do the biogenic emissions account for the differences between

C1 and C2?

*All biogenic emissions are internally calculated and therefore account for all the differences in the emissions between REFC1 and REFC1SD, as clarified above. Figure 1, left top panel, shows all VOC emissions, while the second left top panel shows only the biogenic part of the VOC emissions. As can be seen from that figure, the differences between REFC1 and REFC2 in biogenic emissions are much smaller than between REFC1 and REFC1SD. We add a sentence regarding the cause of the differences in emissions at Page 7, last paragraph:*

*"The emissions differ the most in summer during their peak (Figure 1, bottom row).* ***Despite the fact that surface temperatures in REFC1SD are warmer than in REFC1, more low cloud clouds and reduced solar radiation (as evident in photolysis rates) near the surface may be the important driver for the reduced biogenic emissions in REFC1SD, which has to be further investigated.***

17. P8, L1, "performance". Please rephrase. I think you mean performance of the simulation, not the chemical variables.

*Changed*

18. P8, L13 "N", Do you mean reactive nitrogen (N) including NOx, PAN, N2O etc or ...?

*We looked at NO2 and clarified this in the text. Figure 2 shows NO2 but is in units TgN. We changed the figure accordingly.*

19. P8, L20-22, "Variations in emissions....". This is a very general statement and could be elaborated. In addition to additional information on differences in emissions between the simulations to what extent can it be expected that the dynamics differ? I would assume dynamics between C1 and C2 would be similar over the historical period except for some differences in aerosol forcing. Is this correct? I am not sure what dynamical metric would be most appropriate to show? I would guess convective mass flux might be sensitive to model dynamics.

*To investigate differences in methane lifetime, various effects have to be taken into account and differences in dynamics and convection, but also nudging of the model, may play an important role. All this has to be addressed in a future study.*

20. P8, The differences in ozone are dramatic. The high ozone values (and high OH) are notable in the SD simulation and evidently impact the methane lifetime. Instead of a general statement the authors could dig a bit deeper here – the stratospheric ozone column and lightning NOx do

not seem to explain this difference in ozone. Is O3S the same between the simulations? How about height of convection, or Hadley circulation? It would be helpful if the authors could explain the difference in these simulations more specifically.

*These are interesting questions and will need more investigation, but they are beyond the scope of this paper. We do add at Page 10 Line 12, based on a response to Reviewer 1:*

*"At 250 hPa, which is the UTLS at mid and high latitudes, REFC1SD overestimates ozone by up to 50%, particularly at mid latitudes in both hemispheres.* ***This could be the result of strong mixing in the UTLS associated with the use of the small nudging amount of 1% in this study; however, this needs to be investigated in more detail in future studies.****" The other experiments show smaller deviations from the observations of about 20% or less."*

21. Some more information on the number of ozonesondes that go into the comparison in Figure 3 would be helpful. What does the caption mean by: "12 observed profiles per year and season"? Is it 12 observed profiles per year or per season?

*Changed to "****12 observed profiles per season in a year****".*

22. P9, L25, "Large part to differences. . ..". Really? From Table 1 it the STE of O3 is larger in the SD simulation than the online simulations despite the fact that tropospheric O3S is smaller. Thus, the explanation given here doesn't seem to be correct. Have the authors looked at differences in O3 loss or production between the simulations?

*We agree, that STE difference may not be the largest part of the difference. We also have looked at O3 loss and production for the same regions, and do see differences there as well, and change the sentence to:*

*"Results from REFC1 and REFC2 show larger deviations from the observations than REFC1SD over these two regions.* ***These are in part due to differences in the amount of stratospheric ozone entering the troposphere for the different experiments (see Figure 3, right column, dashed lines), but also due to changes in ozone loss and production, especially in summer.*** *Discrepancies in ozone between the experiments can be explained by differences in O3S for the whole year at 500 hPa and for winter months at 900 hPa. During summer months, differences in chemical production at the surface for the different experiments seem to play an additional role and explain about 5-10 ppb of the deviations for Western Europe."*

23. P10, It is curious that the SD simulation tends to overestimate 250 hPa ozone in the mid and high latitudes but to get about the same STE as the other simulations and to have less O3S in the troposphere. Any explanation?

*Reviewer 1 raised a similar concern, we answered and changed the text (see above):*

*Transport problems in the model may be the likely reason for the overestimation. In follow-on studies, it turns out that the nudging amount of 1% is impacting the convection in REFC1SD in a non optimal way in the troposphere (Jessica Neu, personal communication). A nudging value of 10% is improving ozone values in the UTLS.*

24. Why is Figure A2 not used in the paper itself? It seems this figure could just as easily be included in the main paper.

*We have included a lot of discussion on ozone and there is little new that this figure offers. We added it for completeness in the supplement.*

25. P10, L23. What is the evidence of a transport problem (see comment 22)

*As discussed above, larger differences in O3S do occur in high northern latitudes in winter and spring.*

26. P10, Figure 6. I find it noteworthy that the pole to mid-latitude ozone gradients are rather different in the two experiments, with the SD simulations showing a larger southward ozone gradient which seems to be more consistent with the measurements.

*We change the text to:*

***"Observed features, for example the summertime maximum of ozone over the eastern Mediterranean/Middle East (Kalabokas et al., 2013, Zanis et al., 2014), are reproduced by the REFC1 and REFC1SD experiments. The ozone gradient between mid latitudes and tropics is for the most part well captured, for example over Japan in summer. The pole to mid-latitude ozone gradient in the SD simulation is showing a larger southward ozone gradient than the REFC1 simulation, which is more consistent with the measurements.***
*Regional differences in tropospheric ozone between the different model experiments have to be investigated in future studies."*

27. P10, L32-35. The simulated tropospheric and stratospheric total ozone using 150 hPa as a cut-off is compared to the ozone climatology based on OMI and MLS satellite observations. The authors should address to what extent we might expect an offset (possibly seasonally varying) due to an "apples to oranges" comparison. That is, what is the effect of using the 150 ppb ozone contour as a tropopause in the model versus assumptions made in the measurements? The tropospheric ozone column might be particularly sensitive to assumptions vis-à-vis the tropopause height.

*There are small differences in choosing the tropopause level. However, comparisons between the simulations are based on the same criteria. We change the text to:*

*"**The model tropopause for this diagnostic is defined as the 150 ppb ozone level, which may lead to small differences between observations and model simulations, but not between model experiments themselves**."*

28. P12, L21 "The model reproduces. . .."? Really? This is not all clear from inspecting the figure (which is in a log-scale).

*The uploaded figure had a problem, in particular of the low altitude averages. We include the new figure in the revised manuscript, the model simulations agree somewhat better in mid- to high latitudes. We also change the sentence pointed out by the reviewer to:*

*"The model reproduces BC values in the SH and NH mid latitudes **for most seasons within the range of uncertainty.** "*

29. P12, L23, "The South-to-North gradient is represented well"? Please be more specific. Do you mean the hemispheric gradient? The aerosol burden is not always larger in the N.H. than the S.H. at all heights and months (e.g., September). This section could in general use a more in-depth and precise analysis of the model-measurement comparison for aerosols.

*We think, that most of the important information has been included in the paragraph, and to clarify change the paragraph to:*

*"Otherwise, **in spring and summer**, the **hemispheric** gradient of BC is represented well, following the observed larger burden in the NH compared to the SH, with some overestimation in the SH. The largest BC values in the NH spring are however underestimated. On the other hand, BC values in August/September, and partly November, are overestimated in the NH and in March/April and June/July in the SH."*

30. A recent paper (On the capabilities and limitations of GCCM simulations of summertime regional air quality: A diagnostic analysis of ozone and temperature simulations in the US using CESM CAM-Chem, Brown-Steiner, B.; Hess, P.G.; Lin, M.Y. (2015) Atmospheric Environment vol. 101 p. 134-148) seems to find some of the same discrepancies between specified dynamics and free-running simulations as found here.

*Papers that have used the version CESM1.2.2 or similar updates show similar discrepancies. The paper that discusses those is Tilmes et al., 2015. We are adding this reference to the conclusions.*

# Representation of the Community Earth System Model (CESM1) CAM4-chem within the Chemistry-Climate Model Initiative (CCMI)

S. Tilmes[1], J.-F. Lamarque[1], L. K. Emmons[1], D. E. Kinnison[1], D. Marsh[1], R. R. Garcia[1], A. K. Smith[1], R. R. Neely[1], A. Conley[1], F. Vitt[1], M. Val Martin[2], H. Tanimoto[3], I. Simpson[4], D. R. Blake[4], and N. Blake[4]

[1]National Center for Atmospheric Research, Boulder, Colorado, USA
[2]The University of Sheffield, Sheffield, S1 3JD, UK
[3]National Institute for Environmental Studies, Tsukuba, Ibaraki 305-8506, Japan
[4]University of California, Irvine, CA, USA

*Correspondence to:* S. Tilmes (tilmes@ucar.edu)

**Abstract.** The Community Earth System Model, CESM1 CAM4-chem has been used to perform the Chemistry Climate Model Initiative (CCMI) reference and sensitivity simulations. In this model, the Community Atmospheric Model Version 4 (CAM4) is fully coupled to tropospheric and stratospheric chemistry. Details and specifics of each configuration, including new developments and improvements are described. CESM1 CAM4-chem is a low top model that reaches up to approximately 40 km and uses a horizontal resolution of 1.9 ° latitude and 2.5 ° longitude. For the specified dynamics experiments, the model is nudged to Modern-Era Retrospective Analysis For Research And Applications (MERRA) reanalysis. We summarize the performance of the three reference simulations suggested by CCMI, with a focus on the ~~observed period~~last 15 years of the simulation when most observations are available. Comparisons with ~~elected~~ selected datasets are employed to demonstrate the general performance of the model. We highlight new datasets that are suited for multi-model evaluation studies. Most important improvements of the model are the treatment of stratospheric aerosols and the corresponding adjustments for radiation and optics, the updated chemistry scheme including improved polar chemistry and stratospheric dynamics, and improved dry deposition rates. These updates lead to a very good representation of tropospheric ozone within 20% of values from available observations for most regions. In particular, the trend and magnitude of surface ozone ~~has been~~ is much improved compared to earlier versions of the model. Furthermore, stratospheric column ozone of the Southern Hemisphere in winter and spring is reasonably well represented. All experiments still underestimate CO most significantly in Northern Hemisphere spring and show a significant underestimation of hydrocarbons based on surface observations.

## 1 Introduction

The Chemistry Climate Model Initiative (CCMI) coordinates evaluation and modeling activieties for both tropospheric and stratospheric global chemistry-climate models. The CCMI-1 model experiments include three reference and several sensitivity experiments to evaluate the performance of chemistry-climate models in the troposphere and stratosphere for past and

present conditions between 1960 and 2010 (REFC1 and REFC1SD), and to identify future climate trends between 1960 and 2100 (REFC2) (Eyring et al., 2013). The REFC1SD simulation differs from the REFC1 simulation in that the dynamics are specified from reanalysis. Comprehensive tropospheric and stratospheric chemistry has been integrated into the Community Atmospheric Model Version 4 (CAM4-chem) of the Community Earth System Model (CESM1) and shows a reasonable representation of present-day atmospheric composition in the troposphere (Lamarque et al., 2012; Tilmes et al., 2015) and stratosphere (Lamarque et al., 2010). This model is therefore well suited to participate in the CCMI model intercomparison project.

The purpose of this paper is to summarize the CESM1 CAM4-chem model configurations that were used to perform the reference CCMI model experiments (Section 2) including physics, dynamics, the chemical mechanism and aerosol description, as well as a summary of newly integrated diagnostics. We also describe issues that have been identified after the simulations were performed and their likely impacts. In addition, we summarize the global performance of the model in Section 3, and evaluate selected diagnostics based on observational data sets in Section 4. We employ existing and new datasets to evaluate the general performance of the model. More in-depth analysis and evaluations will follow in multi-model comparison studies. Improvements in comparison to earlier versions of the model are discussed in the Conclusions.

## 2 Model description

CESM is a fully coupled Earth System model, which includes atmosphere, land, ocean, and sea-ice components. All CCMI simulations are carried out with the same model code that is based on CESM version 1.1.1 (CESM1) (Neale et al., 2013), with modifications discussed below. The configuration of the model used here fully couples the Community Atmosphere Model Version 4 (CAM4), the Community Land model Version 4.0 (CLM4.0), the Parallel Ocean Program Version 2 (POP2), and the Los Alamos sea ice model (CICE Version 4). The land model ~~does not include~~ was run without an interactive carbon or nitrogen cycle and only the atmospheric and land components are coupled to the chemistry. The climatological present-day land cover is used for all simulations.

### 2.1 The atmosphere model

Detailed information about the physics of the atmosphere model used here are described in Neale et al. (2013) and Richter and Rasch (2008), and also summarized in Lamarque et al. (2012, and references therein). In summary, deep convection is treated by ~~the Zhang and McFarlanle (1995) scheme, with improvements as described in Richter and Rasch (2008) and Neale et al. (2008).~~ Zhang and McFarlanle (1995) with improvements in the convective momentum transport (Richter and Rasch, 2008), which improved surface winds, stresses, and tropical convection. At the same time, an entraining plume was added to the convection parameterization, which together with the momentum transport improved the representation of El Nino–Southern Oscillation (ENSO) significantly (Neale et al., 2008). The photolysis calculation uses a look-up table between 200 and 750 nm and online calculations for wavelengths $< 200$ nm. Only changes in the ozone column, but not in the aerosol burden, impact photolysis rates. Attenuation of the spectral irradiance above the model top is calculated using the approach of Kinnison et al. (2007) and Lamarque et al. (2012).

Processes in the planetary boundary layer are represented using the Holtslag and Boville (1993) parameterization. Wet deposition of gas and aerosol compounds is based on Neu and Prather (2012), as described in Lamarque et al. (2012). In this version of CAM4-chem all aerosols in the cloudy fraction of the grid cell are assumed to reside within cloud droplets and are removed in proportion to the cloud water removal rate. Aerosols directly impact the radiation and chemistry, but do not change the radiative properties of clouds (i.e., no representation of the aerosol indirect effects is included).

Lightning $NO_x$ is parameterized following Price and Vaughan (1993) and Price et al. (1997). The global amount of produced lightning $NO_x$ is scaled differently for the SD and the FR experiments due to differences in the meteorology to ensure values of approximately 3-5 Tg N/yr for present day conditions.

### 2.1.1 Model grid

For all CCMI reference simulations, CESM1 CAM4-chem uses a horizontal grid with a resolution of 1.9 ° x 2.5 ° (latitude by longitude), and uses the finite volume dynamical core. The top of the model is located at 3 hPa (about 40 km). The vertical coordinate is sigma (hybrid terrain-following pressure) in the troposphere, switching over to isobaric ~~above~~ at pressure levels less than 100 hPa; the vertical resolution of the model depends on the configuration of the experiment. The atmosphere model, CAM4, makes use of 2 different configurations, the free running (FR, with 26 vertical levels) and the specified dynamics (SD, with 56 vertical levels adopted from the analysis fields), see Lamarque et al. (2012). For the SD configuration, internally derived meteorological fields are nudged every time step of 30 minutes by 1% towards reanalysis fields (equivalent to a 50 h Newtonian relaxation time scale for nudging) from Modern-Era Retrospective Analysis For Research And Applications (MERRA) reanalysis (http://gmao.gsfc.nasa.gov/merra/) (Rienecker et al., 2011). Nudged meteorological fields include wind components, temperatures, surface pressure, surface stress, latent, and sensible heat flux. The MERRA reanalysis fields are interpolated to the horizontal resolution of the model prior to running the simulation. The MERRA surface geopotential height is used for the SD simulations to be consistent with the reanalysis fields.

### 2.1.2 Quasi-Biennial Oscillation

The SD configuration of the model incorporates the observed Quasi-Biennial Oscillation (QBO), which is present in the meteorological analysis fields. The limited vertical resolution of the FR model configurations does not allow for the generation of an internal QBO in CAM4-chem. Therefore, for the FR CCMI experiments, REFC1 and REFC2, the QBO is imposed in the model by relaxing equatorial zonal winds between ~~86 hPa and the model top~~ 90 to 3 hPa to the observed interannual variability, following the approach by Matthes et al. (2010). Here, we vary the QBO phase between eastward and westward phase using an approximate 28-month period, similar to what was done by Marsh et al. (2013).

### 2.1.3 Improved gravity wave representation

The representation of sub-gridscale gravity waves (GW) in CAM was formerly limited to orographic gravity waves using the parameterization adapted from ~~?~~McFarlane (1987). In the present simulations, the parameterizations of non-orographic gravity

waves generated by convection (Beres et al., 2005) and fronts (Richter et al., 2010), which were developed for the Whole Atmosphere Community Climate Model (WACCM), are also included.

In addition, we have added another gravity wave module to represent the waves with large horizontal wavelengths that are often observed in the stratosphere (e.g., Zink and Vincent, 2001). The new GW module is adopted from the inertia-gravity wave (IGW) parameterization developed by Xue et al. (2012) for an interactive QBO. The formulation includes the impact of the Coriolis force on gravity wave propagation and breaking. Rather than applying it in the equatorial region, as done by Xue et al. (2012), we use a more general mechanism for determining sources; gravity waves are triggered by the same frontal threshold used for the mesoscale gravity waves (Richter et al., 2010). This has the impact of shifting the bulk of the waves from the tropics to middle and high latitudes. In the current implementation, gravity waves have a narrow phase speed spectrum (-20 to 20 m/s) and long horizontal wavelength (1000 km). The momentum forcing associated with this module particularly impacts the winter stratosphere. In the Southern Hemisphere (SH), it enhances downwelling and increases the winter stratospheric temperature, which in previous simulations was substantially colder than observed.

However, it was found, that the version of the IGW parameterization used for the performed experiments has a narrow IGW spectrum centered on zero phase velocity instead of being centered on the speed of the background wind at the GW launch level, as in the standard GW parameterization. Even with this shortcoming, the model produces a much improved temperature evolution in the stratosphere, in particular in the SH high latitudes compared to earlier versions. This results in a well resolved ozone hole in winter and spring over Antarctica. No significant changes are expected from a corrected IGW parameterization for the troposphere.

#### 2.1.4 Tropospheric aerosols

CAM4-chem runs with the bulk aerosol model (BAM), which simulates the distribution of externally-mixed sulfate, black carbon (BC), primary organic carbon (OC), sea-salt and dust, as described in Lamarque et al. (2012). The dust emissions are calibrated so that the global dust aerosol optical depth (AOD) is about 0.025 to 0.030 (Mahowald et al., 2006). The distribution of sea-salt and dust are described using four size bins. In CAM4-chem, the formation of secondary organic aerosols (SOA) is coupled to the chemistry and biogenic emissions. SOA are derived using the 2-product model approach using laboratory determined yields for SOA formation from monoterpene, isoprene and aromatic photooxidation, as described in Heald et al. (2008). The aging process of BC and OC from hydrophobic to hydrophilic is included through a specified conversion timescale. For all aerosol species, the size distributions are specified as in Lamarque et al. (2012). Aerosols interact with the gas-phase chemistry through heterogeneous reactions that depend on the available surface area density (SAD), as discussed below. For the tropospheric SAD calculation, sulfate, hydrophilic black carbon~~and~~, primary organic carbon, and nitrates are included, where SOA has not been included. This may lead to a significant underestimation of tropospheric SAD in the experiments.

#### 2.1.5 Representation of aerosols in the stratosphere

Aerosol mass, heating rates and SAD are revised in this version compared to earlier configurations. Most significantly, the model uses a new stratospheric aerosol and SAD dataset, derived based on observations, to force models participating in

CCMI (Eyring et al., 2013). In addition, in order to fully utilize the aerosol size information provided by the new model input file, the optics in the radiative transfer code associated with CAM4 (i.e., CAMRT) (Neale and al., 2010) have been modified to include a lookup table for aerosol effective radius in the shortwave radiation scheme. The new description leads to an updated representation of volcanic heating for REFC1 and REFC2, whereas in REFC1SD volcanic heating is included through the nudged temperature fields. See ~~Neely et al. (2015, in prep.)~~ Neely et al. (2015) for a full description of changes to the stratospheric aerosol scheme. Tropospheric aerosols that enter the stratosphere are promptly removed (as listed in Table A2) since the aerosol burden in the stratosphere is prescribed.

#### 2.1.6 Coupling to the land model

Dry deposition velocity for tracers in the atmosphere are calculated online in ~~CLM~~CLM4.0. An updated calculation is used, where leaf and stomatal resistances are coupled to the leaf area index (LAI) and are also linked to the photosynthesis provided by the land model, as described ~~by~~ in Val Martin et al. (2014).

Biogenic emissions are calculated online in CLM using the Model of Emissions of Gases and Aerosols from Nature (MEGAN), version 2.1 (Guenther et al., 2012). ~~The~~ An erroneous implementation of MEGAN in this version differs from the description of Guenther et al. (2012) by using the LAI from the previous model timestep (30 minutes) instead of the average of the previous 10 days~~, and by~~. In addition, in this version we are using a fixed $CO_2$ mixing ratio, instead of the simulated atmospheric value, in the calculation of the $CO_2$ inhibition effect on isoprene emissions. The corrected implementation is closer to the algorithm of Guenther et al. (2012).

### 2.2 Chemical mechanism ~~and aerosol description~~

The chemical mechanism of CAM4-chem includes 169 species, listed in Table A1. Depending on the chemical lifetime of each species, an explict or semi-implicit solver is used. Emissions of gas-phase and aerosol species, as indicated in Table A1, are in general distributed at the surface. Only aircraft emissions of BC and nitrogen dioxide, and volcanic emissions of sulfur and sulfate, are vertically distributed. Species with lower boundary conditions, listed in Table A1, as discussed in Section 2.3.2. Different species experience wet and/or dry deposition, as also listed in Table A1. Furthermore, 14 artificial tracers are implemented as recommended by CCMI ~~(Eyring et al., 2013)~~(Eyring et al., 2013, Section 4.2.1): $NH_5$, $NH_{50}$, $NH_{50W}$, $AOA_{NH}$, $ST80_{25}$, $CO_{25}$, $CO_{50}$, $SO_{2t}$, SF6em, $O_3S$, E90, $E90_{NH}$, $E90_{SH}$. $O_3S$ is a stratospheric ozone tracer that represents the amount of ozone in the troposphere with its source in the stratosphere. $O_3S$ is set to stratospheric values at the tropopause, and experiences the same loss rates as ozone in the troposphere, as defined by CCMI. ~~Following~~ As interpreted from the CCMI recommendation, dry deposition is not included, which will lead to an overestimation of $O_3S$ in the lower boundary layer when compared to ozone (which is dry deposited).

The chemical mechanism, is based on the Model for Ozone and Related chemical Tracers (MOZART), version 4 mechanism for the troposphere (Emmons et al., 2010). It further includes extended stratospheric chemistry (Kinnison et al., 2007) and updates, as described in Lamarque et al. (2012) and Tilmes et al. (2015). The reactions include photolysis, gas-phase chemistry, and heterogeneous chemistry, in both troposphere and stratosphere. ~~Furthermore, tropospheric aerosols that enter the~~

~~stratosphere are promptly removed, since the aerosol burden in the stratosphere is prescribed.~~ The complete chemical mechanism is listed in Table A2 and incorporates all the latest updates. All aerosols and some gas-phase species, including $H_2O$, $O_2$, $CO_2$, $O_3$, $N_2O$, $CH_4$, CFC11, CFC12, are radiatively active.

Reaction rates are updated following JPL2010 recommendations (Sander et al., 2011). Bromoform ($CHBr_3$) and dibromomethane ($CH_2Br_2$) were added to the model to represent the stratospheric bromine loading from very short lived (VSL) species. The surface volume mixing ratio for these two VSL species was set globally to 1.2 ppt (i.e., 6 ppt total bromine). This approach adds an additional $\approx$ 5 ppt of inorganic bromine to the stratosphere. The resulting stratospheric total inorganic bromine abundance (for present day conditions) from both long-lived and VSL species is $\approx$ 21.5 ppt. Besides the current Lower Boundary Condition (LBC) approach for VSL species, ~~CAM4-Chem~~ CAM4-chem can be also configured with a Full-VSL mechanism, including detailed gas-phase halogen chemistry mechanism, geographically and time-dependent distributed sources of 9 halocarbons and improved representation of heterogeneous recycling and removal rates in the troposphere (Fernandez et al., 2014; Saiz-Lopez et al., 2014).

Details on updated reactions and processes for chemistry in the polar stratosphere are described in Wegner et al. (2013) and Solomon et al. (2015).

~~Lightning is parameterized following Price and Vaughan (1993); Price et al. (1997). The global amount of produced lightning is scaled differently for the SD and the FR experiments due to differences in the meteorology to ensure values of approximately 3-5 Tg N/yr for present day conditions.~~

Diagnostics of the tropospheric ozone production and loss rates are explicitly calculated, see Table A3, in adding the listed reaction rates r of two species A and B, r(A-B), as well as the photolysis reaction of ONITR (defined as lumped organic nitrate species that includes nitrates derived from the OH- and $NO_3$-initiated oxidation of isoprene and terpenes, and related species), called jonitr:

$$\begin{aligned} O3-Prod =& r(NO-HO2)+r(CH3O2-NO)+r(PO2-NO)+r(CH3CO3-NO)+ \\ & r(C2H5O2-NO)+.92*r(ISOPO2-NO)+r(MACRO2-NOa)+r(MCO3-NO)+ \\ & r(C3H7O2-NO)+r(RO2-NO)+r(XO2-NO)+.9*r(TOLO2-NO)+ \\ & r(TERPO2-NO)+.9*r(ALKO2-NO)+r(ENEO2-NO)+r(EO2-NO)+ \\ & r(MEKO2-NO)+0.4*r(ONITR-OH)+jonitr \end{aligned}$$

$$\begin{aligned} O3-Loss =& r(O1D-H2O)+r(OH-O3)+r(HO2-O3)+r(C3H6-O3)+ \\ & .9*r(ISOP-O3)+r(C2H4-O3)+.8*r(MVK-O3)+0.8*r(MACR-O3)+ \\ & r(C10H16-O3) \end{aligned}$$

These are defined based on the rate-limiting terms for the gas phase reactions of the $O_x$ family ($O_3$, O, ~~O1D~~$O_1D$ , $NO_2$), not including $O_2 + h\nu \rightarrow 2O$ production, $O_x$, $ClO_x$, and $BrO_x$ losses, and are therefore not valid for the stratosphere. The sum of those rates are very similar to the explicit calculation of the net chemical change of ozone (as listed in Table A2).

### 2.3 Experimental Setup

The reference experiments are set up according to the CCMI recommendation, including surface and altitude dependent emissions, and lower boundary conditions. The three reference experiments are performed with the recommended emissions~~; for~~ . REFC1 and REFC1SD (years 1960-2010), use the same emissions, excluding biogenic emissions. Anthropogenic and biomass burning emissions are from the MACCity emission data set ~~(Granier et al., 2011), while for~~ and change every year (Granier et al., 2011). For REFC2 ~~,~~ (years 1960-2100), anthropogenic and biomass burning emissions are taken from AR5 (Eyring et al., 2013) (see Figure A1)~~.~~ , which only vary every 5-10 years. All emissions include a seasonal cycle. Biogenic emissions are calculated every timestep by MEGAN, as described in Section 2.1.6.

The REFC1SD experiment is nudged to analyzed air temperatures, winds, surface fluxes, and surface pressure, and uses the Hadley Centre Global Sea Ice and Sea Surface Temperature ~~(HadISST~~Version 2 (HadISST2) observed time-dependent data set for sea surface temperatures (SSTs) and sea ice. The REFC1 experiment also uses prescribed SSTs and sea ice, while the REFC2 simulation calculates temperatures in the ocean and atmosphere. We have carried out one simulation for REFC1SD, and an ensemble of three members for each REFC1 and REFC2.

The solar cycle is prescribed using observed daily fields for the years until 2010. For the future period in REFC2, we follow the CCMI recommendation and repeat a sequence of the last four solar cycles (20-23), as defined in http://solarisheppa.geomar.de/ccmi.

#### 2.3.1 Initial conditions and spin-up

CAM4-chem initial conditions for the three REFC1 and REFC2 ensemble members are taken from 3 realizations of CESM1-WACCM 20th Century ensemble for CMIP5 (Marsh et al., 2013). The spin-up period started in 1950 and ran ~~until~~ through 1959. The experiments simulated the years 1960 to 2010 (REFC1) and 1960 to 2100 (REFC2). Initial conditions for the REFC1SD simulation are taken from the first REFC1 ensemble member in 1975. The spin-up of this experiment covered the years 1975 to 1979, repeating 1979 meteorological analysis for each year. The experiment was performed between 1980 and 2010.

#### 2.3.2 Lower boundary conditions

For all of the three reference experiments the same monthly and annually varying lower boundary conditions are used based on the Representation Concentration Pathway 6.0 (RCP6.0) Coupled Model Intercomparison Project Phase 5 (CMIP5) future projection (Taylor et al., 2012). We prescribe $CO_2$, $N_2O$, $CH_4$, as well as the following halogen species based on the CCMI recommendations: $CCl_4$, $CF_2ClBr$, $CF_3Br$, CFC11, CFC113, CFC12, $CH_3Br$, $CH_3CCl_3$, $CH_3Cl$, $H_2$, HCFC22, CFC114, CFC115, HCFC141b, HCFC142b, $CH_2Br_2$, $CHBr_3$, H1202, H2402, $SF_6$. A North-South gradient was added for $CH_3Br$,

HCFC22, HCFC141b, HCFC142b, based on the HIAPER (High-Performance Instrumented Airborne Platform for Environmental Research) Pole-to-Pole Observations (HIPPO) (Wofsy et al., 2011), (Mijeong Park, pers. comm.).

## 3 Model performance

### 3.1 Global diagnostics

The general state of the model is investigated by comparing diagnostics of globally averaged values between different model experiments that are averaged between 1995 and 2010 (Table 1). The global surface temperatures (TS) of all three experiments are in agreement within 0.15 K for the observed period (Table 1). REFC1SD land temperature (TS land) is on average 0.25 K higher than for REFC1 and 0.15 K higher than for the REFC2 experiments (Table 1). The largest deviations occur over high latitudes (not shown). In the REFC1SD experiment, low cloud fraction is significantly larger than in the other experiments, which results in a much smaller shortwave cloud forcing (SWCF) of -83 W/m$^2$ compared the other experiments that are with 54-56 W/m$^2$ more in line with observations.

Differences in clouds and land surface temperatures between the reference experiments result in different biogenic emissions of volatile organic components (VOCs) (Figure 1). REFC1SD biogenic emissions are about 10% lower than ~~derived~~ in the REFC1 experiment and about 15% lower than in the REFC2 experiment. The emissions differ the most in summer during their peak (Figure 1, bottom row). Despite the fact that surface temperatures in REFC1SD are warmer than in REFC1, more low cloud clouds and reduced solar radiation (as evident in photolysis rates) near the surface may be the important driver for the reduced biogenic emissions in REFC1SD, which has to be further investigated. Other differences in the REFC1 and REFC2 VOC emissions arise from different anthropogenic and biomass burning emissions, while biogenic emissions differ by less than 10% (Table 1). Despite the variation in the reference experiments, biogenic emissions are in agreement with earlier estimates (e.g., Young et al., 2012).

The performance of the model in simulating tropospheric chemical variables (Table 1) is similar to earlier studies (e.g., Tilmes et al., 2015). Methane lifetime is low compared to observational estimates of ~~11.3~~11.2 years (Prather et al., 2012). Ozone budgets, including ozone burden, stratosphere troposphere exchange, and budgets of carbon monoxide (CO), are in agreement with earlier model studies (Young et al., 2012). Aerosol burdens of primary organic matter (POM) and secondary organic aerosols (SOA) are low, but within the spread of other model results (Tsigaridis et al., 2014). The $SO_4$ burden with 0.45 to 0.51 TgS and the lifetime of 3.0 to 3.5 days is somewhat low compared to the Aerocom multi-model mean of 0.66 TgS and 4.12 days, respectively (e.g., Liu et al., 2012). The dust optical depth ~~is with~~ around 0.04 is somewhat higher than suggested by Mahowald et al. (2006).

### 3.2 Trends of tropospheric components

Time varying emissions of ozone precursors and aerosols impact the oxidation capacity of the atmosphere. In the following, we discuss the evolution of different chemical species and surface area density in the tropical troposphere between 30° S–30° N,

tropospheric methane lifetime, and stratospheric column ozone (Figure 2), since methane is mostly controlled by processes in the Tropics. Increasing nitrogen ~~(N~~dioxide ($NO_2$), CO and VOC burdens between 1960 and 1990 result in increasing tropospheric ozone with the strongest trend between 1960 and 1990. Increasing aerosols between 1960 and 1990 result in an increase in SAD, with little change after 1990. Together with the increase in CO burden, this results in a decrease of OH. ~~On the other hand,~~ Other factors result in an increase in tropospheric OH, including decreasing stratospheric column ozone between 1960 and 2010, ~~and increasing column ozone combined with the increasing nitrogen oxides~~ increasing tropospheric column ozone, increasing nitrogen dioxides ($NO_x$) burden~~and methane emissions, increases tropospheric OH~~ , and decreasing methane emissions (e.g., Murray et al., 2014). Both counteracting effects on OH result in little change in methane lifetime between 1960 and 1990. After 1990, SAD, as well as CO and VOC trends are leveling off, but nitrogen dioxide and ozone burdens are still increasing, partly due to increasing lightning $NO_x$ production (not shown). This results in a decreasing trend in methane lifetime after 1990 for all reference experiments.

The burden of chemical tracers differ between REFC1SD and REFC1/ REFC2 (Figure 2). Variations in emissions and atmospheric dynamics, including surface temperature, clouds, and convection, influence the chemical composition of the atmosphere. Exchange processes between the upper troposphere and lower stratosphere are also different in the model experiments and impact ozone. ~~For instance,~~ The shorter lifetime of methane in REFC1SD compared to the other experiments may be a result of a reduction in high clouds, and, to some amount, the larger ozone mixing ratios in the ~~upper troposphere~~tropical troposphere, which would increase the oxidation capacity in the ~~REFC1SD experiment results in a higher oxidation capacity of the troposphere and therefore a shorter lifetime of methane compared to the other experiments~~tropics. This has to be investigated in more detail in future studies.

Besides a continuous decrease, the stratospheric ozone column shows a significant drop after major volcanic eruptions (e.g., WMO, 2006). This is expected due to an increase in stratospheric SAD after the eruption, which causes enhanced halogen activation, resulting in ozone depletion (see Figure 2).

## 4 Evaluation against selected diagnostics

The purpose of this section is to give an overview of selected variables and diagnostics that summarize the performance of the model, including some of its shortcomings, in comparison to observations. Additional and more detailed investigations are expected in future multi-model comparison studies. We only discuss the performance of the reference experiments for past and present day. Model results from other sensitivity studies are not analyzed and will be discussed in future studies.

### 4.1 Ozone

Ozone is an important atmospheric tracer in both the troposphere and the stratosphere. In the troposphere and at the surface, ozone is an air pollutant and is impacted by various precursors, most importantly CO and $NO_x$. A reasonable performance of tropospheric ozone is required for air quality studies. In the stratosphere, ozone is strongly influenced by dynamics, photochemistry, and catalytic reactions (e.g., WMO, 2010). The strength of the transport of stratospheric ozone into the troposphere

follows a seasonal cycle controlled by the Brewer Dobson circulation (BDC). Shortcomings in the representation of the strength of the BDC and mixing processes between stratosphere and troposphere influence the performance of tropospheric ozone, as discussed below. In addition, ozone is an important greenhouse gas in the upper troposphere and lower stratosphere (UTLS) and influences tropospheric climate (e.g., WMO, 2014)).

#### 4.1.1 Trends and seasonality of ozone

Ozone trends and seasonality in the reference experiments are compared to ozonesonde observations (Tilmes et al., 2012) in the free troposphere (at 500 hPa) and the boundary layer (at 900 hPa). For Japan, we employ an additional climatology derived by Tanimoto et al. (2015), which is based on surface observations at five marine boundary layer sites from the Acid Deposition Monitoring Network in East Asia (EANET) for ~~altitudes below~~ pressure levels larger than 900 hPa, and a combination of the historical Measurements of OZone~~and water vapour~~, water vapour, carbon monoxide and nitrogen oxides by in-service ~~Aircraft~~ AIrbus airCraft (MOZAIC, URL: http://www.iagos.fr/mozaic) data (over Narita airport) and ozonesonde observations (at Tateno/Tsukuba) for ~~altitudes~~ pressure levels between 472 and 616 hPa. We use an artificial stratospheric ozone tracer ($O_3S$) to identify differences in stratosphere troposphere exchange (STE) between different model experiments for four selected regions (see Figures 3 and 4).

In high northern latitudes, REFC1SD reproduces the magnitude and trend of ozone very well, including variability within the standard deviation of the observations for all seasons, as shown in the example of the Northern Hemisphere (NH) Polar West region (Figure 3, first and second row). A very good agreement between the model experiment and ozonesondes also exists for Western Europe, with exception of the high bias between October and February at 500 hPa of 5-10 ppb (Figure 3, third and fourth row).

Results from REFC1 and REFC2 show larger deviations from the observations than REFC1SD over these two regions~~, which are due in large part~~. These are in part due to differences in the amount of stratospheric ozone entering the troposphere for the different experiments (see Figure 3, right column, dashed lines), but also due to changes in ozone loss and production. Discrepancies in ozone between the experiments can be explained by differences in $O_3S$ for the whole year at 500 hPa and for winter months at 900 hPa. During summer months, differences in chemical production at the surface for the different experiments seem to play an additional role and explain about 5-10 ppb of the deviations for Western Europe.

Selected ozonesondes over Eastern US and Japan are located further south and are more strongly influenced by tropical air masses and tropospheric intrusion in the lowermost stratosphere in particular in winter, as discussed in Tilmes et al. (2012). Each of the regions covers only two stations and so uses fewer observations for the different years than other regions, which increases the uncertainty of trends (Saunois et al., 2012).

Comparisons for Eastern US and Japan are illustrated in Figure 4. For Japan, we are using two datasets to compare to model results. Ozone mixing ratios and trends at 900 hPa over Japan using ozonesondes, as compiled by Tilmes et al. (2012), Figure 4 (black diamonds), largely differ from the climatology by Tanimoto et al. (2015), which is based on surface observations (black triangles). This is due to uncertainties in the ozonesonde observations at these altitudes, which should be treated with caution. On the other hand, the two climatologies agree well in the free troposphere at 500 hPa.

For Eastern US and Japan the REFC1SD model experiment nicely reproduces the observed trend and magnitude of ozone within the variability of the observations at 900 hPa. The seasonal cycle for both regions are well reproduced. This significant improvement compared to earlier versions of the model is in part a result of the improved calculation of dry deposition rates, as discussed in Val Martin et al. (2014) over the ~~U. S. .~~ US. REFC1 ~~/~~and REFC2 experiments show slightly larger values at 900 hPa in comparison to the REFC1SD experiment particularly in winter, aligned with a larger $O_3$ contribution from the stratosphere, as determined by the $O_3S$ tracer (see Figure 4). At 500 hPa, ozone mixing ratios and trends are well reproduced for all experiments in summer. However, the model overestimates winter ozone mixing ratios in the upper troposphere.

#### 4.1.2 Present-day ozone

A comparison with ozonesonde observations over different regions for simulated years between 1995-2010 is presented in Figure 5. Besides some differences in ozone compared to observations, as discussed above, all model experiments reproduce observed tropospheric ozone within ~~about 20%~~ 25% for most of the regions. At 250 hPa, which is the UTLS at mid and high latitudes, REFC1SD overestimates ozone by up to 50%, particularly at mid latitudes in both hemispheres~~, while the~~ . This could be the result of strong mixing in the UTLS associated with the use of the small nudging amount of 1% in this study; however, this needs to be investigated in more detail in future studies. The other experiments show smaller deviations from the observations of about 20% or less. Tropical values at 50 hPa are overestimated by no more than 20% compared to observations for all the experiments, while ozone in the mid and high latitudes in the stratosphere agrees within 10% with observations.

Model results further agree well with HIPPO aircraft observations for profiles sampled from 85° N–65° S over the Pacific Ocean between 2009 and 2011 (Figure A2). In REFC1SD, lower troposphere values (1-2 km) are within the range of the observations, while for REFC1 and REFC2 ozone is overestimated by about 5 ppb in high northern latitudes, in particular in winter and spring, which points to a transport problem as discussed above. Some differences, especially at higher altitudes (7-8 km) are likely caused by the specific meteorological situation for the flight conditions compared to the climatological model results.

The regional performance of tropospheric ozone in the model is further illustrated in Figure 6, comparing simulated ozone mixing ratios with ozone sondes and various aircraft ~~observations~~ nbservations at 3-7 km, as compiled in Tilmes et al. (2015). ~~Besides the described differences between REFC1 and REFC1SD experiments, observed~~ Observed features, for example the summertime maximum of ozone over eastern Mediterranean/Middle East (Kalabokas et al., 2013; Zanis et al., 2014), are reproduced by the ~~model~~REFC1 and REFC1SD experiments. The ozone gradient between mid latitudes and tropics is ~~to~~ for the most part well captured, for example over Japan in summer. The pole to mid-latitude ozone gradient in the SD simulation is showing a larger southward ozone gradient than the REFC1 simulation, which is more consistent with the measurements. Regional differences in tropospheric ozone between the different model experiments have to be investigated in future studies.

We further perform comparisons of model results to a present day ozone climatology based on OMI and MLS satellite observations between 2004 and 2010, compiled by Ziemke et al. (2011), in the troposphere (Figure 7) and stratosphere (Figure 8). The model tropopause for this diagnostic is defined ~~at~~ as the 150 ppb ozone level, which may lead to small differences between observations and model simulations, but not between model experiments themselves. The comparisons reveal additional char-

acteristics of the model performance compared to observations. Tropospheric column ozone is reproduced within ± 10 DU of the observations, with a close agreement to the satellite climatology within less than ± 5 DU in low and mid latitudes in spring and summer (Figure 7). All model experiments show a low bias in mid latitudes in the SH and high bias by 10-15 DU in the NH mid latitudes in winter and fall. NH tropospheric ozone is in general large in the REFC1 and REFC2 simulations compared to the REFC1SD experiments, as discussed above.

Stratospheric ozone in all model experiments agree within ± 30 DU in mid and low latitudes compared to the satellite climatology (Figure 8). Larger deviations from the observations occur in the NH mid and high latitudes in winter and spring with a high bias of up to 60 DU. Ozone in the SH is within about 25 DU from the observations and is reasonably well reproduced by all model experiments, especially for the free running experiments.

### 4.2 Carbon Monoxide

Carbon monoxide, non-methane hydrocarbons and nitrogen dioxides are the most important precursors to the formation of tropospheric ozone. Carbon monoxide also impacts the oxidation capacity of the atmosphere and therefore methane lifetime. We compare the CO burden from different experiments to monthly and zonally averaged tropospheric column carbon monoxide derived from Measurements of Pollution in The Troposphere (MOPITT) Version 6 Level 3 satellite observations, as described in Tilmes et al. (2015) (see Figure 9). The climatological averaging kernel and a priori is applied to both observations and model experiments in the same way.

The most obvious difference between observations and model results occurs in NH winter and spring. All model experiments are biased low by about a third relative to observations, similar to result from the Atmospheric Chemistry and Climate Model Intercomparison Project (ACCMIP) (Naik et al., 2013; Lamarque et al., 2012). In summer and fall, the CO representation differs between different experiments, in agreement with differences in biogenic emissions. The lowest CO burden is simulated for the REFC1SD experiment, which also shows the lowest emissions of VOCs in summer (see Figure 1). This may translate into lower CO values in fall. Furthermore, the tropospheric OH burden is significantly larger in REFC1SD compared to the other experiments (not shown), which is consistent with more ozone in the tropical troposphere (see Figure 2).

Simulated CO column in the tropics agree with the satellite climatology within the interannual variability. However, the model ~~underestimate~~ underestimates CO column in the SH for all the experiments, in particular in summer. In contrast, comparisons to HIPPO CO in-situ observations indicate very good agreement between CO mixing ratios in the SH over the remote region of the Pacific Ocean for most of the seasons (see Figure A3). Furthermore, CO mixing ratios are largely underestimated in March and April in comparison to the aircraft observations, consistent with the satellite comparison. Differences in CO will be investigated in more detail in future studies.

### 4.3 Hydrocarbons

Hydrocarbons are important tropospheric compounds that are emitted from vegetation, biomass burning and anthropogenic sources, including oil and gas extraction activities. They are important ozone precursors, influence the oxidation capacity of the atmosphere, and eventually form CO.

Ethane and other hydrocarbons have been measured using canister samples along coastal and island sites in the Pacific Ocean since 1984 typically every three months, December, March, June and September (Simpson et al., 2012); data are available at http://cdiac.ornl.gov/trends/otheratg/blake/blake.html. We have compiled a climatology using ethane mixing ratios between 1995 and 2010 that covers latitudes between 50° S and 75° N (shown in Figure 10). Comparisons to the three model experiments reveal a very large underestimation of ethane mixing ratios by up to ~~5 times~~ 80% in spring. The smallest deviations occur in NH fall. These deviations are likely contributing to the underestimation of CO and overestimation of OH.

While there is significant uncertainty in the speciation of VOC emissions (e.g., Li et al., 2014), which could lead to this discrepancy, it is likely there is an underestimation of all VOC emissions. Globally, ethane concentrations have been declining since long-term global record-keeping began. Simpson et al. (2012) reported a 21% decline in global ethane concentrations from 1984 to 2010, which is much smaller than the discrepancy between the model and observations.

### 4.4 Aerosols

A reasonable description of aerosols in climate models, including interactions with chemistry and clouds, is important for the representation of radiative processes. The aerosol optical depth, global aerosol burden of organic matter, black carbon, and sulfate aerosol, are global diagnostics to evaluate the general performance of aerosol processes (Table 1). This version of CAM4-chem produces values for these diagnostics very similar to earlier model studies using CAM4-chem (e.g., Tilmes et al., 2015). Here, we focus on the evaluation of background black carbon in comparison to HIPPO observations. The HIPPO campaign between 2009 and 2011 provided a comprehensive data set of black carbon over the remote region ~~over~~ of the Pacific. Black carbon results from the model are averaged over the same locations, and altitude levels and compared to the observations, as described above.

All model simulations show a very similar distribution (Figure 11), with only a few deviations from each other mostly in the SH. The model reproduces BC values in the SH and NH mid latitudes for most seasons within the range of uncertainty. A significant high bias in BC occurs in the tropics for all altitude levels and most seasons. Otherwise, ~~the South-to-North~~ in spring and summer, the hemispheric gradient of BC is represented well, following the observed larger burden in the NH compared to the SH~~in March/April and June/July~~, with some overestimation in the SH. The largest BC values in the NH spring are however underestimated. On the other hand, BC values in August/September, and partly November, are overestimated in the NH and in March/April and June/July in the SH.

## 5 Conclusions

The CESM1 CAM4-chem model has been used to perform the CCMI reference and sensitivity simulations. This paper provides an overview of the model setup of the reference experiments, including a detailed description of new developments. The most important improvements of the model beyond what has been discussed in earlier studies (Lamarque et al., 2012; Tilmes et al., 2015) are the treatment of stratospheric aerosols and the corresponding radiation and optics, which is important for the free running experiments (Neely et al., 2015). Further, the chemistry scheme has been updated to reaction rates of JPL 2010, and

improved polar chemistry has been implemented (Wegner et al., 2013; Solomon et al., 2015). A new gravity wave description, while implemented incorrectly in the code, led to an improved representation of the evolution of polar stratospheric ozone in the SH. The updated dry deposition scheme by Val Martin et al. (2014) resulted in a much improved ozone near the surface, as also shown in Tilmes et al. (2015), and leads to a very good representation of ozone mixing ratios and trends in the REFC1SD simulation.

Global model diagnostics are ~~investiaged~~ investigated and a selected evaluation of key chemical species, including ozone, carbon monoxide, hydrocarbons, and black carbon is performed. We limit our evaluation to present day results of the REFC1SD, REFC1 and REFC2 experiments. Comparisons to observations are focused mostly on the troposphere. Nevertheless, stratospheric column ozone reproduces observed values, in particular in SH winter and spring, but overestimates values in the NH high latitudes.

For the troposphere, near surface ozone mixing ratios and trends are very well reproduced and within ~~20~~25% of the values from ozonesonde and satellite observations throughout the troposphere. A high bias in mid and high northern latitudes for the REFC1 and REFC2 experiments can be explained by a stronger influence of stratospheric air masses compared to the REFC1SD simulation. This points to shortcomings in the stratosphere to troposphere exchange in the free running simulations. On the other hand, the specified dynamics model experiment shows an overestimation of ozone in mid latitude UTLS, as well as enhanced ozone in the upper tropical troposphere compared to the free running experiments. The impact of shortcomings in the dynamical description of the model needs to be investigated in multi-model comparison studies.

Some biases in the model have not been resolved compared to earlier versions of the model (e.g., Tilmes et al., 2015). CO is still biased low in all model experiments in the NH, especially in spring. Some differences between the experiments may be ~~ascribed~~ attributed to differences in biogenic emissions. Correspondingly, methane lifetime is ~~rather~~ low compared to observational estimates, which is likely related to shortcomings in emissions, but also to too ~~great~~ large an oxidation capacity of the atmosphere. Significant shortcomings of hydrocarbons (shown for ethane) are identified in particular in the NH. The ~~North-to-South~~ hemispheric gradient of BC in the model is reproduced well in most seasons, while the fall and winter values in mid latitudes are often overestimated in mid latitudes. BC in the Tropics is largely overestimated for most seasons. This points to potential shortcomings in emissions, but also loss processes in the model.

## 6 Code and data availability

The model code of the documented simulations is based on the Community Earth System Model, CESM version 1.1.1 (CESM1), http://www.cesm.ucar.edu/models/cesm1.1/index.html. Modifications to the model code will be documented at http://www2.cesm.ucar.edu/models/scientifically-supported. The data of the simulations are available for download at the NCAR Earth System Grid (ESG) (https://www.earthsystemgrid.org/home.html ) and are submitted to the BADC database for the CCMI project.

*Acknowledgements.* We thank the HIPPO team for performing reliable aircraft observations used in this study. MERRA data used in this study have been provided by the Global Modeling and Assimilation Office (GMAO) at NASA Goddard Space Flight Center through the NASA GES DISC online archive. The CESM project is supported by the National Science Foundation and the Office of Science (BER) of the US Department of Energy. The National Center for Atmospheric Research is funded by the National Science Foundation.

## References


Beres, J. H., Garcia, R. R., Boville, B. a., and Sassi, F.: Implementation of a gravity wave source spectrum parameterization dependent on the properties of convection in the Whole Atmosphere Community Climate Model (WACCM), Journal of Geophysical Research D: Atmospheres, 110, 1–13, doi:10.1029/2004JD005504, 2005.

Emmons, L. K., Walters, S., Hess, P. G., Lamarque, J.-F., Pfister, G. G., Fillmore, D., Granier, C., Guenther, A., Kinnison, D., Laepple, T., Orlando, J., Tie, X., Tyndall, G., Wiedinmyer, C., Baughcum, S. L., and Kloster, S.: Description and evaluation of the Model for Ozone and Related chemical Tracers, version 4 (MOZART-4), Geosci. Model Dev., 3, 43–67, doi:10.5194/gmd-3-43-2010, 2010.

Eyring, V., Lamarque, J.-F., and Hess, P.: Overview of IGAC/SPARC Chemistry-Climate Model Initiative (CCMI) Community Simulations in Support of Upcoming Ozone and Climate Assessments, Tech. rep., doi:SPARC Newsletter No. 40, p. 48-66, 2013, 2013.

Fernandez, R. P., Salawitch, R. J., Kinnison, D. E., Lamarque, J.-F., and Saiz-Lopez, a.: Bromine partitioning in the tropical tropopause layer: implications for stratospheric injection, Atmospheric Chemistry and Physics Discussions, 14, 17 857–17 905, doi:10.5194/acpd-14-17857-2014, http://www.atmos-chem-phys-discuss.net/14/17857/2014/, 2014.

Granier, C., Bessagnet, B., Bond, T., D'Angiola, A., Denier van der Gon, H., Frost, G. J., Heil, A., Kaiser, J. W., Kinne, S., Klimont, Z., Kloster, S., Lamarque, J.-F., Liousse, C., Masui, T., Meleux, F., Mieville, A., Ohara, T., Raut, J.-C., Riahi, K., Schultz, M. G., Smith, S. J., Thompson, A., van Aardenne, J., van der Werf, G. R., and van Vuuren, D. P.: Evolution of anthropogenic and biomass burning emissions of air pollutants at global and regional scales during the 1980–2010 period, Climatic Change, 109, 163–190, doi:10.1007/s10584-011-0154-1, http://link.springer.com/10.1007/s10584-011-0154-1, 2011.

Guenther, a. B., Jiang, X., Heald, C. L., Sakulyanontvittaya, T., Duhl, T., Emmons, L. K., and Wang, X.: The Model of Emissions of Gases and Aerosols from Nature version 2.1 (MEGAN2.1): an extended and updated framework for modeling biogenic emissions, Geoscientific Model Development, 5, 1471–1492, doi:10.5194/gmd-5-1471-2012, http://www.geosci-model-dev.net/5/1471/2012/, 2012.

Heald, C. L., Henze, D. K., Horowitz, L. W., Feddema, J., Lamarque, J.-F., Guenther, a., Hess, P. G., Vitt, F., Seinfeld, J. H., Goldstein, a. H., and Fung, I.: Predicted change in global secondary organic aerosol concentrations in response to future climate, emissions, and land use change, Journal of Geophysical Research: Atmospheres, 113, n/a–n/a, doi:10.1029/2007JD009092, http://doi.wiley.com/10.1029/2007JD009092, 2008.

Holtslag, A. and Boville, B. A.: Local versus nonlocal boundary-layer diffusion in a global climate model, Journal of Climate, 6, 1825–1842, 1993.

Kalabokas, P. D., Cammas, J.-P., Thouret, V., Volz-Thomas, a., Boulanger, D., and Repapis, C. C.: Examination of the atmospheric conditions associated with high and low summer ozone levels in the lower troposphere over the eastern Mediterranean, Atmospheric Chemistry and Physics, 13, 10 339–10 352, doi:10.5194/acp-13-10339-2013, http://www.atmos-chem-phys.net/13/10339/2013/, 2013.

Kinnison, D. E., Brasseur, G. P., Walters, S., Garcia, R. R., Marsch, D. A., Sassi, F., Boville, B. A., Harvey, V. L., Randall, C. E., Emmons, L., Lamarque, J. F., Hess, P., Orlando, J. J., Tie, X. X., Randel, W., Pan, L. L., Gettelman, A., Granier, C., Diehl, T., Niemaier, U., and Simmons, A. J.: Sensitivity of chemical tracers to meteorological parameters in the MOZART-3 chemical transport model, J.Geophys. Res., 112, D20 302, doi:10.1029/2006JD007879, 2007.

Lamarque, J.-F., Bond, T. C., Eyring, V., Granier, C., Heil, a., Klimont, Z., Lee, D., Liousse, C., Mieville, a., Owen, B., Schultz, M. G., Shindell, D., Smith, S. J., Stehfest, E., Van Aardenne, J., Cooper, O. R., Kainuma, M., Mahowald, N., McConnell, J. R., Naik, V., Riahi, K., and van Vuuren, D. P.: Historical (1850–2000) gridded anthropogenic and biomass burning emissions of reactive

gases and aerosols: methodology and application, Atmospheric Chemistry and Physics, 10, 7017–7039, doi:10.5194/acp-10-7017-2010, http://www.atmos-chem-phys.net/10/7017/2010/, 2010.

Lamarque, J.-F., Emmons, L. K., Hess, P. G., Kinnison, D. E., Tilmes, S., Vitt, F., Heald, C. L., Holland, E. A., Lauritzen, P. H., Neu, J., Orlando, J. J., Rasch, P. J., and Tyndall, G. K.: CAM-chem: description and evaluation of interactive atmospheric chemistry in the Community Earth System Model, Geoscientific Model Development, 5, 369–411, doi:10.5194/gmd-5-369-2012, http://www.geosci-model-dev.net/5/369/2012/, 2012.

Li, M., Zhang, Q., Streets, D. G., He, K. B., Cheng, Y. F., Emmons, L. K., Huo, H., Kang, S. C., Lu, Z., Shao, M., Su, H., Yu, X., and Zhang, Y.: Mapping Asian anthropogenic emissions of non-methane volatile organic compounds to multiple chemical mechanisms, Atmospheric Chemistry and Physics, 14, 5617–5638, doi:10.5194/acp-14-5617-2014, http://www.atmos-chem-phys.net/14/5617/2014/, 2014.

Liu, X., Easter, R. C., Ghan, S. J., Zaveri, R., Rasch, P., Shi, X., Lamarque, J.-F., Gettelman, a., Morrison, H., Vitt, F., Conley, a., Park, S., Neale, R., Hannay, C., Ekman, a. M. L., Hess, P., Mahowald, N., Collins, W., Iacono, M. J., Bretherton, C. S., Flanner, M. G., and Mitchell, D.: Toward a minimal representation of aerosols in climate models: description and evaluation in the Community Atmosphere Model CAM5, Geoscientific Model Development, 5, 709–739, doi:10.5194/gmd-5-709-2012, http://www.geosci-model-dev.net/5/709/2012/, 2012.

Mahowald, N. M., Yoshioka, M., Collins, W. D., Conley, A. J., Fillmore, D. W., and Coleman, D. B.: Climate response and radiative forcing from mineral aerosols during the last glacial maximum, pre-industrial, current and doubled-carbon dioxide climates, Geophysical Research Letters, 33, 2–5, doi:10.1029/2006GL026126, 2006.

Marsh, D. R., Mills, M. J., Kinnison, D. E., Lamarque, J.-F., Calvo, N., and Polvani, L. M.: Climate Change from 1850 to 2005 Simulated in CESM1(WACCM), Journal of Climate, 26, 7372–7391, doi:10.1175/JCLI-D-12-00558.1, http://journals.ametsoc.org/doi/abs/10.1175/JCLI-D-12-00558.1, 2013.

Matthes, K., Marsh, D. R., Garcia, R. R., Kinnison, D. E., Sassi, F., and Walters, S.: Role of the QBO in modulating the influence of the 11 year solar cycle on the atmosphere using constant forcings, Journal of Geophysical Research: Atmospheres, 115, 1–17, doi:10.1029/2009JD013020, 2010.

McFarlanle, N. A.: The effect of orographically excited wave drag on the general circulation of the lower stratosphere and troposphere, J. Aerosol Sci., 44, 175–1800, 1987.

Murray, L. T., Mickley, L. J., Kaplan, J. O., Sofen, E. D., Pfeiffer, M., and Alexander, B.: Factors controlling variability in the oxidative capacity of the troposphere since the Last Glacial Maximum, Atmospheric Chemistry and Physics, 14, 3589–3622, doi:10.5194/acp-14-3589-2014, http://www.atmos-chem-phys.net/14/3589/2014/, 2014.

Naik, V., Voulgarakis, A., Fiore, A. M., Horowitz, L. W., Lamarque, J.-F., Lin, M., Prather, M. J., Young, P. J., Bergmann, D., Cameron-Smith, P. J., Cionni, I., Collins, W. J., Dalsø ren, S. B., Doherty, R., Eyring, V., Faluvegi, G., Folberth, G. A., Josse, B., Lee, Y. H., MacKenzie, I. A., Nagashima, T., van Noije, T. P. C., Plummer, D. A., Righi, M., Rumbold, S. T., Skeie, R., Shindell, D. T., Stevenson, D. S., Strode, S., Sudo, K., Szopa, S., and Zeng, G.: Preindustrial to present-day changes in tropospheric hydroxyl radical and methane lifetime from the Atmospheric Chemistry and Climate Model Intercomparison Project (ACCMIP), Atmospheric Chemistry and Physics, 13, 5277–5298, doi:10.5194/acp-13-5277-2013, http://www.atmos-chem-phys.net/13/5277/2013/, 2013.

Neale, R. and al., E.: Description of the NCAR Community Atmosphere Model (CAM 4.0), Tech. rep., NCAR/TN-485+STR, NCAR TECHNICAL NOTE, 2010.

Neale, R. B., Richter, J. H., and Jochum, M.: The impact of convection on ENSO: From a delayed oscillator to a series of events, Journal of Climate, 21, 5904–5924, doi:10.1175/2008JCLI2244.1, http://journals.ametsoc.org/doi/abs/10.1175/2008JCLI2244.1, 2008.

Neale, R. B., Richter, J., Park, S., Lauritzen, P. H., Vavrus, S. J., Rasch, P. J., and Zhang, M.: The Mean Climate of the Community Atmosphere Model (CAM4) in Forced SST and Fully Coupled Experiments, Journal of Climate, 26, 5150–5168, doi:10.1175/JCLI-D-12-00236.1, http://journals.ametsoc.org/doi/abs/10.1175/JCLI-D-12-00236.1, 2013.

Neely, R., Conley, A., Vitt, F., Kinnison, D. E., and Lamarque, J. F.: A Scheme for Consistently Prescribing Volcanic Aerosol to the Radiation and Chemistry Models of CESM1, Geosci. Model Dev. Discuss., 8, 10711–10734, doi:10.5194/gmdd-8-10711-2015, 2015.

Neu, J. L. and Prather, M. J.: Toward a more physical representation of precipitation scavenging in global chemistry models: cloud overlap and ice physics and their impact on tropospheric ozone, Atmospheric Chemistry and Physics, 12, 3289–3310, doi:10.5194/acp-12-3289-2012, http://www.atmos-chem-phys.net/12/3289/2012/, 2012.

Prather, M. J., Holmes, C. D., and Hsu, J.: Reactive greenhouse gas scenarios: Systematic exploration of uncertainties and the role of atmospheric chemistry, Geophysical Research Letters, 39, n/a–n/a, doi:10.1029/2012GL051440, http://doi.wiley.com/10.1029/2012GL051440, 2012.

Price, C., Penner, J., and Prather, M. J.: NOx from lightning: 1. Global distribution based on lightning physics, Journal of Geophysical Research: Atmospheres, 102, 5929–5941, 1997.

Price, J. D. and Vaughan, G.: The potential for stratosphere-troposphere exchange in cut-off-low systems, Q.˜J.˜R. Meteorol. Soc., 119, 343–365, 1993.

Richter, J. and Rasch, P. J.: Effects of convective momentum transport on the atmospheric circulation in the Community Atmosphere Model, Version 3, J. Climate, 21, 1487–1499, doi:http://dx.doi.org/10.1175/2007JCLI1789.1, 2008.

Richter, J. H., Sassi, F., and Garcia, R. R.: Toward a Physically Based Gravity Wave Source Parameterization in a General Circulation Model, Journal of the Atmospheric Sciences, 67, 136–156, doi:10.1175/2009JAS3112.1, 2010.

Rienecker, M. M., Suarez, M. J., Gelaro, R., Todling, R., Bacmeister, J., Liu, E., Bosilovich, M. G., Schubert, S. D., Takacs, L., Kim, G.-K., Bloom, S., Chen, J., Collins, D., Conaty, A., and et al. da Silva: MERRA - NASA's Modern-Era Retrospective Analysis for Research and Applications, J. Climate, 24, 3624–3648, doi:10.1175/JCLI-D-11-00015, 2011.

Saiz-Lopez, a., Fernandez, R. P., Ordóñez, C., Kinnison, D. E., Gómez Martín, J. C., Lamarque, J.-F., and Tilmes, S.: Iodine chemistry in the troposphere and its effect on ozone, Atmos. Chem. Phys. Discuss., 14, 19 985–20 044, doi:10.5194/acpd-14-19985-2014, http://www.atmos-chem-phys-discuss.net/14/19985/2014/$\delimiter"026E30F$nhttp://www.atmos-chem-phys-discuss.net/14/19985/2014/acpd-14-1 2014.

Sander, S. P., Friedl, R. R., Barker, J. R., Golden, D. M., Kurylo, M. J., Sciences, G. E., Wine, P. H., Abbatt, J. P. D., Burkholder, J. B., Kolb, C. E., Moortgat, G. K., Huie, R. E., and Orkin, V. L.: Chemical Kinetics and Photochemical Data for Use in Atmospheric Studies Evaluation Number 17 NASA Panel for Data Evaluation, JLP Publ., 10-6, 2011.

Saunois, M., Emmons, L., Lamarque, J.-F., Tilmes, S., Wespes, C., Thouret, V., and Schultz, M.: Impact of sampling frequency in the analysis of tropospheric ozone observations, Atmospheric Chemistry and Physics, 12, 6757–6773, doi:10.5194/acp-12-6757-2012, http://www.atmos-chem-phys.net/12/6757/2012/, 2012.

Simpson, I. J., Sulbaek Andersen, M. P., Meinardi, S., Bruhwiler, L., Blake, N. J., Helmig, D., Rowland, F. S., and Blake, D. R.: Long-term decline of global atmospheric ethane concentrations and implications for methane, Nature, 488, 490–494, doi:10.1038/nature11342, http://dx.doi.org/10.1038/nature11342, 2012.

Solomon, S., Kinnison, D., Bandoro, J., and Garcia, R.: Journal of Geophysical Research : Atmospheres Simulation of polar ozone depletion : An update, Journal of Geophysical Research D: Atmospheres, pp. 7958–7974, doi:10.1002/2015JD023365.Received, 2015.

Tanimoto, H., Zbinden, R. M., Thouret, V., and Nedelec, P.: Consistency of tropospheric ozone observations by different platforms and techniques in the global databases, Tellus˜B, 2015.

Taylor, K. E., Stouffer, R. J., and Meehl, G. A.: An Overview of CMIP5 and the experiment design, Bulletin of the American Meteorological Society, 93, 485–498, doi:10.1175/BAMS-D-11-00094.1, http://journals.ametsoc.org/doi/abs/10.1175/BAMS-D-11-00094.1, 2012.

Tilmes, S., Lamarque, J.-F., Emmons, L. K., Conley, a., Schultz, M. G., Saunois, M., Thouret, V., Thompson, a. M., Oltmans, S. J., Johnson, B., and Tarasick, D.: Technical Note: Ozonesonde climatology between 1995 and 2011: description, evaluation and applications, Atmospheric Chemistry and Physics, 12, 7475–7497, doi:10.5194/acp-12-7475-2012, http://www.atmos-chem-phys.net/12/7475/2012/, 2012.

Tilmes, S., Lamarque, J.-F., Emmons, L. K., Kinnison, D. E., Ma, P.-L., Liu, X., Ghan, S., Bardeen, C., Arnold, S., Deeter, M., Vitt, F., Ryerson, T., Elkins, J. W., Moore, F., Spackman, J. R., and Val Martin, M.: Description and evaluation of tropospheric chemistry and aerosols in the Community Earth System Model (CESM1.2), Geoscientific Model Development, 8, 1395–1426, doi:10.5194/gmd-8-1395-2015, http://www.geosci-model-dev.net/8/1395/2015/, 2015.

Tsigaridis, K., Daskalakis, N., Kanakidou, M., Adams, P. J., Artaxo, P., Bahadur, R., Balkanski, Y., Bauer, S. E., Bellouin, N., Benedetti, a., Bergman, T., Berntsen, T. K., Beukes, J. P., Bian, H., Carslaw, K. S., Chin, M., Curci, G., Diehl, T., Easter, R. C., Ghan, S. J., Gong, S. L., Hodzic, a., Hoyle, C. R., Iversen, T., Jathar, S., Jimenez, J. L., Kaiser, J. W., Kirkevå g, a., Koch, D., Kokkola, H., Lee, Y. H., Lin, G., Liu, X., Luo, G., Ma, X., Mann, G. W., Mihalopoulos, N., Morcrette, J.-J., Müller, J.-F., Myhre, G., Myriokefalitakis, S., Ng, N. L., O'Donnell, D., Penner, J. E., Pozzoli, L., Pringle, K. J., Russell, L. M., Schulz, M., Sciare, J., Seland, O., Shindell, D. T., Sillman, S., Skeie, R. B., Spracklen, D., Stavrakou, T., Steenrod, S. D., Takemura, T., Tiitta, P., Tilmes, S., Tost, H., van Noije, T., van Zyl, P. G., von Salzen, K., Yu, F., Wang, Z., Zaveri, R. a., Zhang, H., Zhang, K., Zhang, Q., and Zhang, X.: The AeroCom evaluation and intercomparison of organic aerosol in global models, Atmospheric Chemistry and Physics, 14, 10 845–10 895, doi:10.5194/acp-14-10845-2014, http://www.atmos-chem-phys.net/14/10845/2014/, 2014.

Val Martin, M., Heald, C. L., and Arnold, S. R.: Coupling dry deposition to vegetation phenology in the Community Earth System Model : Implications for the simulation of surface O 3, Geophys. Res. Lett., pp. 1–9, doi:10.1002/2014GL059651.Received, 2014.

Wegner, T., Kinnison, D. E., Garcia, R. R., and Solomon, S.: Simulation of polar stratospheric clouds in the specified dynamics version of the whole atmosphere community climate model, Journal of Geophysical Research: Atmospheres, 118, 4991–5002, doi:10.1002/jgrd.50415, 2013.

WMO: Executive summary: Scientific assessment of ozone depletion: 2006, Geneva, Switzerland, 2006, Released by WMO and UNEP on 18 August 2006.

WMO: Scientific Assessment of Ozone Depletion, www.unep.ch/ozone/AssessmentPanels/SAP/ScientificAssessment2010/00-SAP-2010-Assement-repo 2010.

WMO: Scientific assessment of ozone depletion: 2014, Global Ozone Research and Monitoring Project-Report No.\ 51, Geneva, Switzerland, 2014.

Wofsy, S. C., , and the HIPPO team: HIAPER Pole-to-Pole Observations (HIPPO): fine-grained, global-scale measurements of climatically important atmospheric gases and aerosols., Philosophical transactions. Series A, Mathematical, physical, and engineering sciences, 369, 2073–86, doi:10.1098/rsta.2010.0313, http://www.ncbi.nlm.nih.gov/pubmed/21502177, 2011.

Xue, X. H., Liu, H. L., and Dou, X. K.: Parameterization of the inertial gravity waves and generation of the quasi-biennial oscillation, Journal of Geophysical Research: Atmospheres, 117, 1–14, doi:10.1029/2011JD016778, 2012.

Young, P. J., Archibald, a. T., Bowman, K. W., Lamarque, J.-F., Naik, V., Stevenson, D. S., Tilmes, S., Voulgarakis, a., Wild, O., Bergmann, D., Cameron-Smith, P., Cionni, I., Collins, W. J., Dalsø ren, S. B., Doherty, R. M., Eyring, V., Faluvegi, G., Horowitz, L. W., Josse, B., Lee, Y. H., MacKenzie, I. a., Nagashima, T., Plummer, D. a., Righi, M., Rumbold, S. T., Skeie, R. B., Shindell, D. T., Strode, S. a., Sudo, K., Szopa, S., and Zeng, G.: Pre-industrial to end 21st century projections of tropospheric ozone from the Atmospheric Chemistry and Climate Model Intercomparison Project (ACCMIP), Atmospheric Chemistry and Physics Discussions, 12, 21 615–21 677, doi:10.5194/acpd-12-21615-2012, 2012.

Zanis, P., Hadjinicolaou, P., Pozzer, a., Tyrlis, E., Dafka, S., Mihalopoulos, N., and Lelieveld, J.: Summertime free-tropospheric ozone pool over the eastern Mediterranean/Middle East, Atmospheric Chemistry and Physics, 14, 115–132, doi:10.5194/acp-14-115-2014, http://www.atmos-chem-phys.net/14/115/2014/, 2014.

Zhang, G. J. and McFarlanle, N. A.: Sensitivity of climate simulations to the parameterization of cumulus convection in the Canadian Climate Centre General Circulation Model, Atmosphere-Ocean, 33, 407–446, 1995.

Ziemke, J. R., Chandra, S., Labow, G. J., Bhartia, P. K., Froidevaux, L., and Witte, J. C.: A global climatology of tropospheric and stratospheric ozone derived from Aura OMI and MLS measurements, Atmospheric Chemistry and Physics, 11, 9237–9251, doi:10.5194/acp-11-9237-2011, http://www.atmos-chem-phys.net/11/9237/2011/, 2011.

Zink, F. and Vincent, R. a.: Wavelet analysis of stratospheric gravity wave packets over Macquarie Island: 1. Wave parameters, Journal of Geophysical Research, 106, 10 275, doi:10.1029/2000JD900847, 2001.

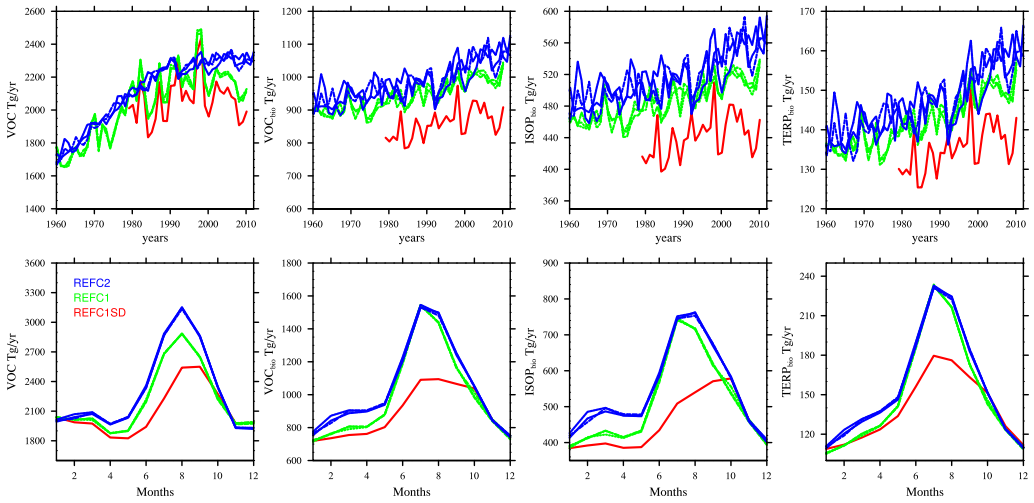


**Figure 1.** Global averaged surface emissions of total volatile organic compounds (VOCs) (first column), biogenic VOCs (second column), biogenic isoprene (third column), and biogenic terpenes (fourth column), for different experiments, REFC1SD (red), REFC1 (green), REFC2 (blue). The seasonal cycle of zonal averages between 1960 and 2010 are shown at the bottom row.

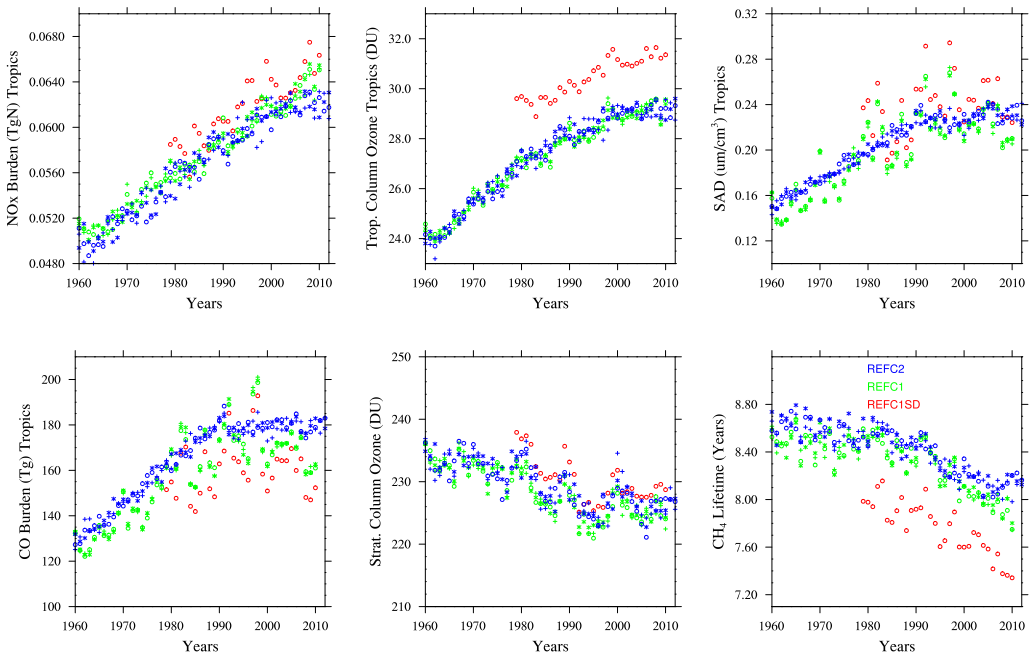


**Figure 2.** Timeseries of annually averaged column integrated tropospheric and tropical nitrogen dioxide (in Tg N), tropospheric ozone burden, and CO, in (30° S–30° N), tropical average of tropospheric surface area density, global stratospheric column ozone, and tropospheric methane lifetime.

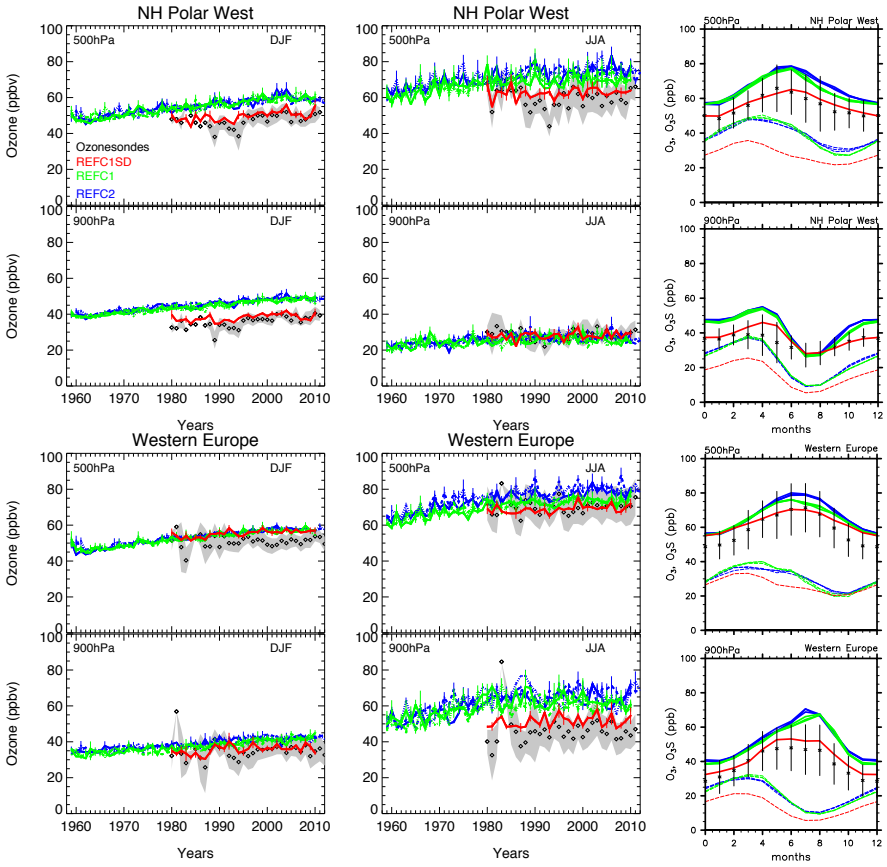


**Figure 3.** Left and middle column: Time evolution of seasonal averaged and regionally aggregated ozone mixing ratios derived from ozone soundings (black diamonds) and model results (colored lines) at two different pressure levels, two different seasons (DJF: left, JJA: right) and regions (NH Polar West, and Western Europe). Grey shading indicates the standard deviation of the observations that include at least 12 observed profiles per ~~year and~~ season in a year. Colored error bars indicate the standard deviation based on monthly-averaged model output. Right column: Regionally aggregated seasonal cycle comparisons of ozone soundings (black lines) and model simulations (colored lines), averaged between 1995 and 2010. Dashed lines indicate mixing ratios of the stratopsheric ozone tracer (see text for more details).

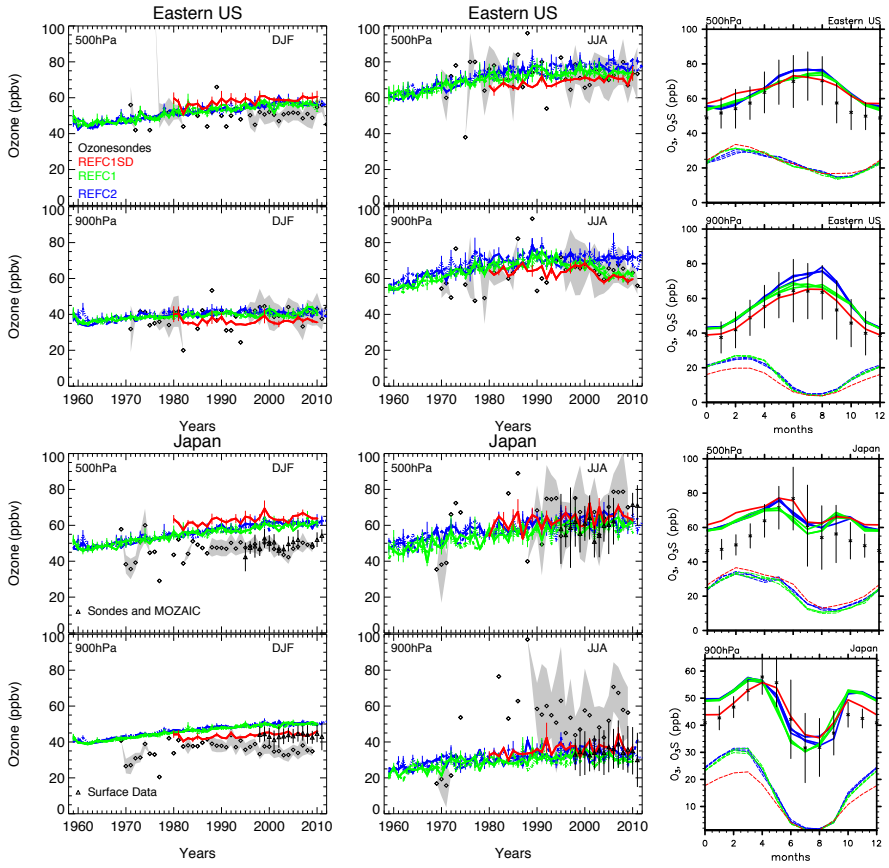


**Figure 4.** As Figure 3, but for Eastern US and Japan instead. For Japan, ozone timeseries compiled by Tanimoto et al. (2015) are added (black triangles) (see text for more details) and used to compare with the seasonal cycle of the model for Japan.

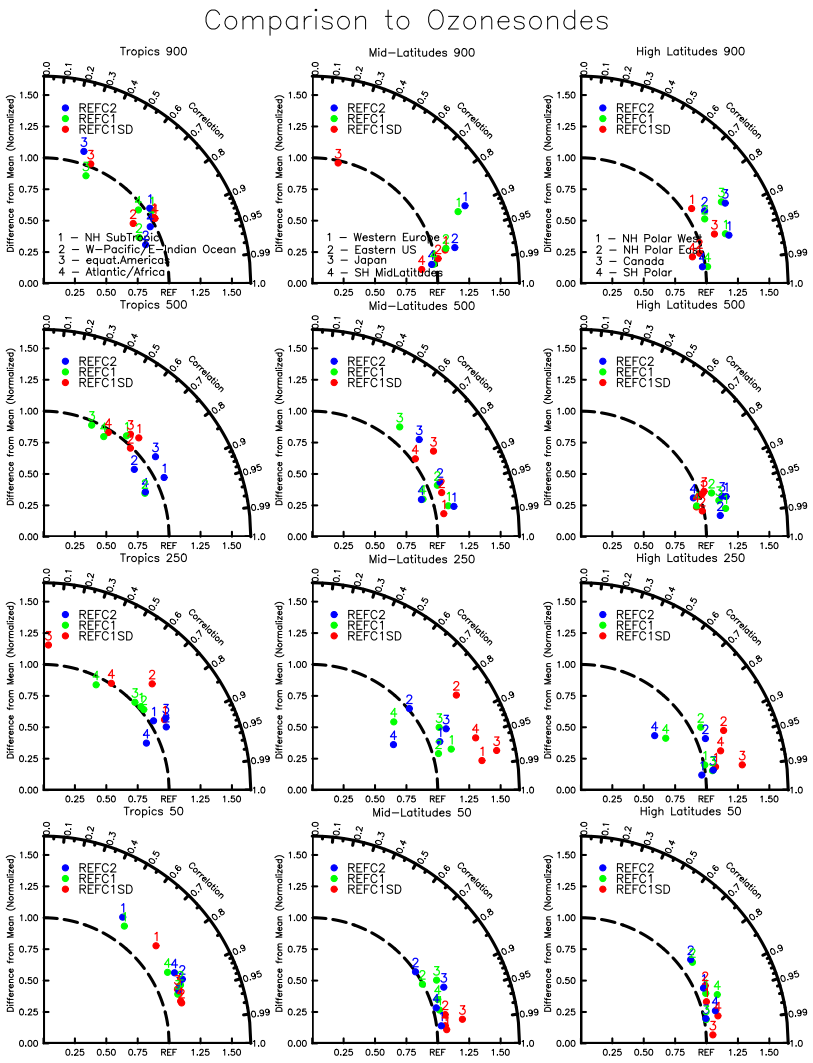


**Figure 5.** Taylor-like diagram comparing the mean and correlation of the seasonal cycle between observations using a present-day ozonesonde climatology between 1995–2011 and model results between 1995–2010, interpolated to the same locations as sampled by the observations and for different pressure levels, 900 hPa (top panel), 500 hPa (second panel), 250 hPa (third panel), and 50 hPa (bottom panel). Different numbers correspond to a specific region, as defined in Tilmes et al. (2012). Left panels: 1 – NH-Subtropics; 2 – W-Pacific/East Indian Ocean; 3 – equat. Americas; 4 – Atlantic/Africa. Middle panels: 1 – Western Europe; 2 – Eastern US; 3 – Japan; 4 – SH Mid-Latitudes. Right panels: 1 – NH Polar West; 2 – NH Polar East; 3 – Canada; 4 – SH Polar.

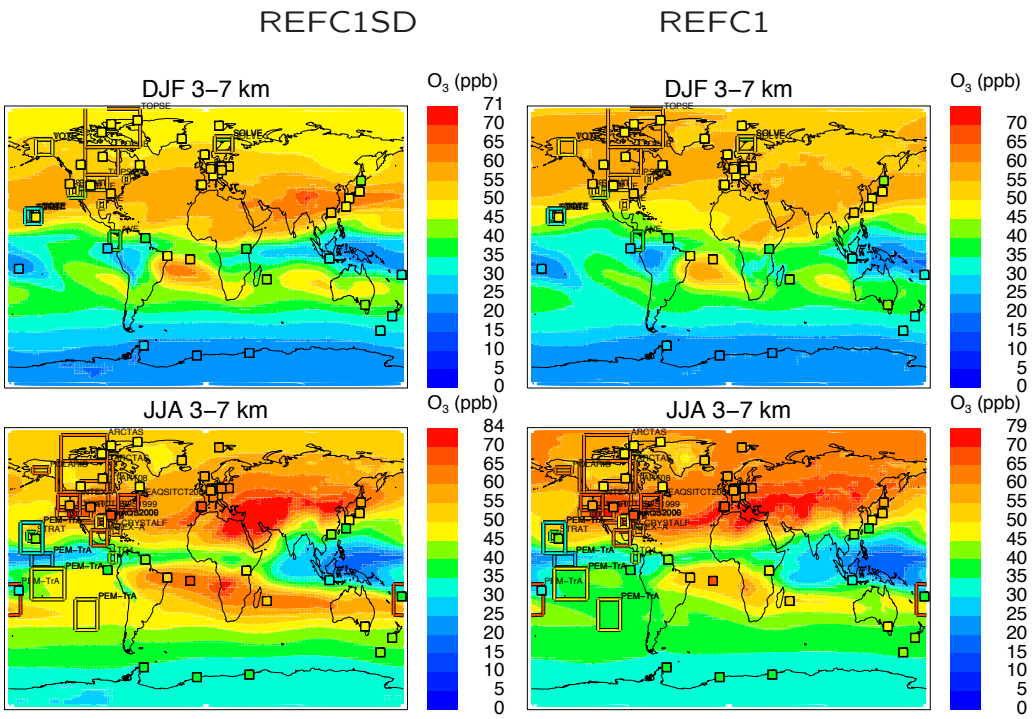


**Figure 6.** Comparison between model results in contours (REFC1SD left and REFC1.1 right) and observations of ozone mixing ratios, averaged over 3-7km for December/January/February (DJF), top, and June/July/August (JJA), bottom. The color of each square represents the value of the observed ozonesonde measurement for the same period and altitude interval, and the color of framed regions corresponds to values derived from aircraft observations averaged over the particular region for each experiment (Tilmes et al., 2015).

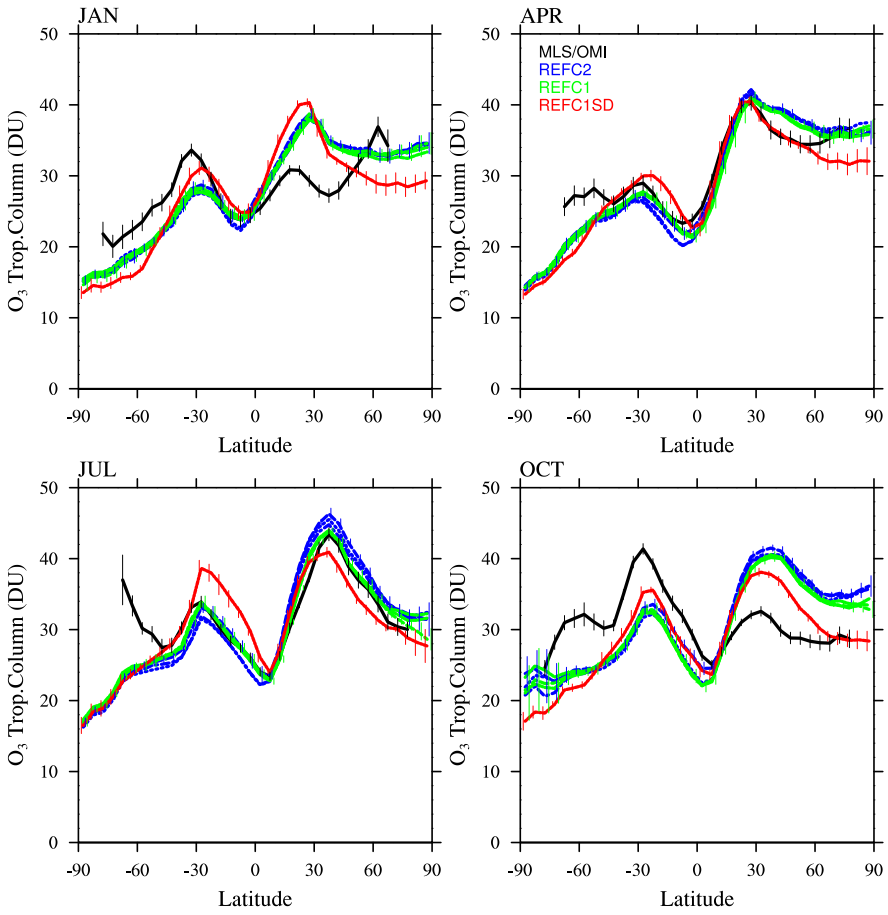


**Figure 7.** Monthly and zonally averaged tropospheric ozone column (in DU) comparison between OMI/MLS observations (black) and different model experiments, see legend, (for ozone $<$ 150 ppb in the model), for four months. Error bars describe the zonally averaged 2 sigma six-year root mean square standard error of the mean at a giving grid point, derived from the 10° N to 10° S gridded product (Ziemke et al., 2011). Model results are interpolated to the same grid and error bars indicate the standard deviation of the interannual variability per latitude interval.

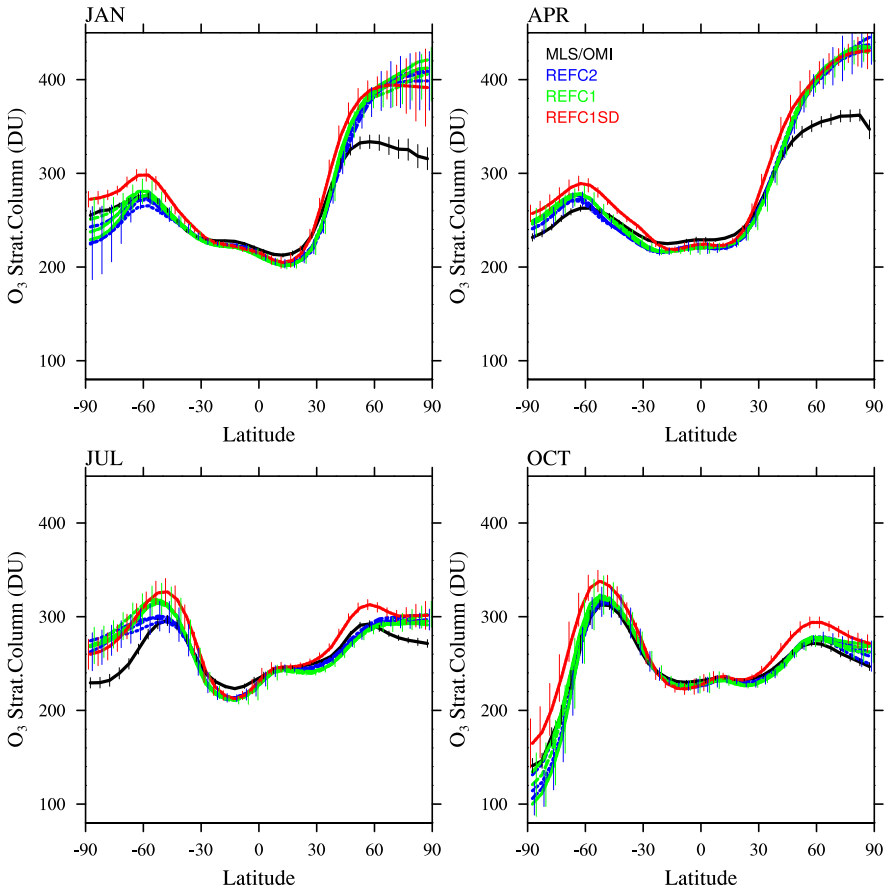


**Figure 8.** As Figure 7, but showing monthly and zonally averaged stratospheric ozone column comparison between OMI/MLS observations (black) and different model experiments, see legend, (for ozone $>$ 150 ppb in the model), for four months.

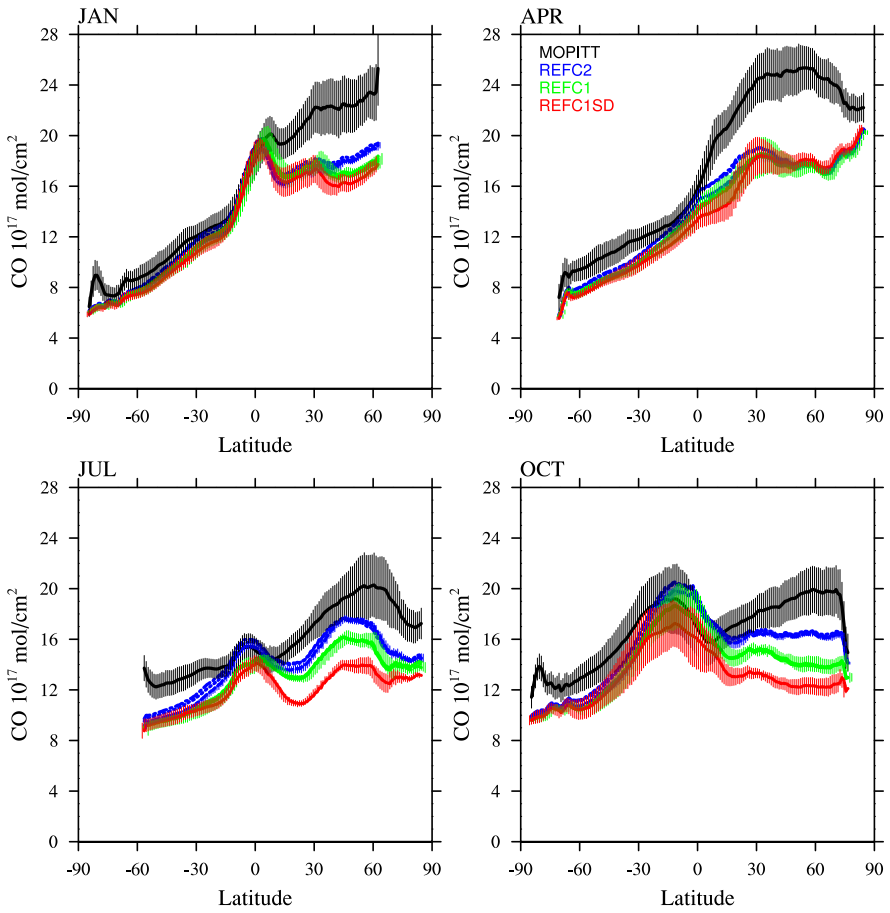


**Figure 9.** Monthly and zonally averaged tropospheric CO column comparison (in molec./cm$^2$) between MOPITT satellite observations (black) and different model experiments, see legend, (for ozone $< 150$ ppb in the model), for four months. Error bars for observations and model experiments show the standard deviation of the interannual variability per latitude interval.

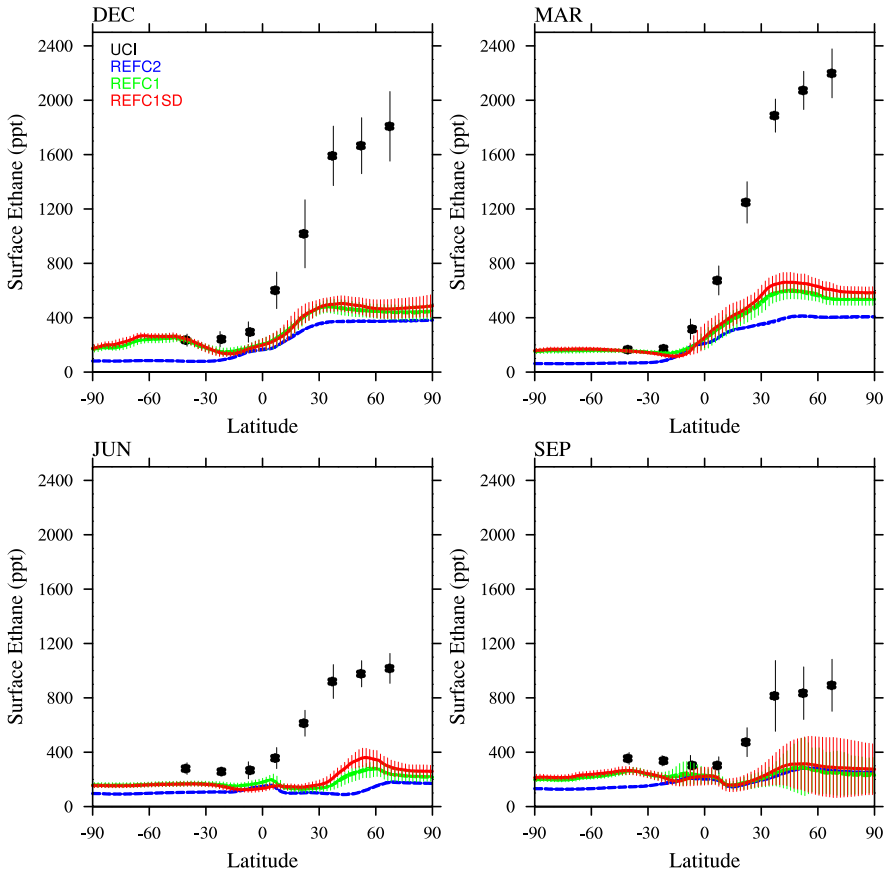


**Figure 10.** Comparison of observed and modeled surface ethane ($C_2H_6$) mixing ratios in each season averaged over 1995-2010 along the length of the Pacific Ocean. Monthly mean CAM4-chem ethane mixing ratios at 190 East are shown for the three model experiments.

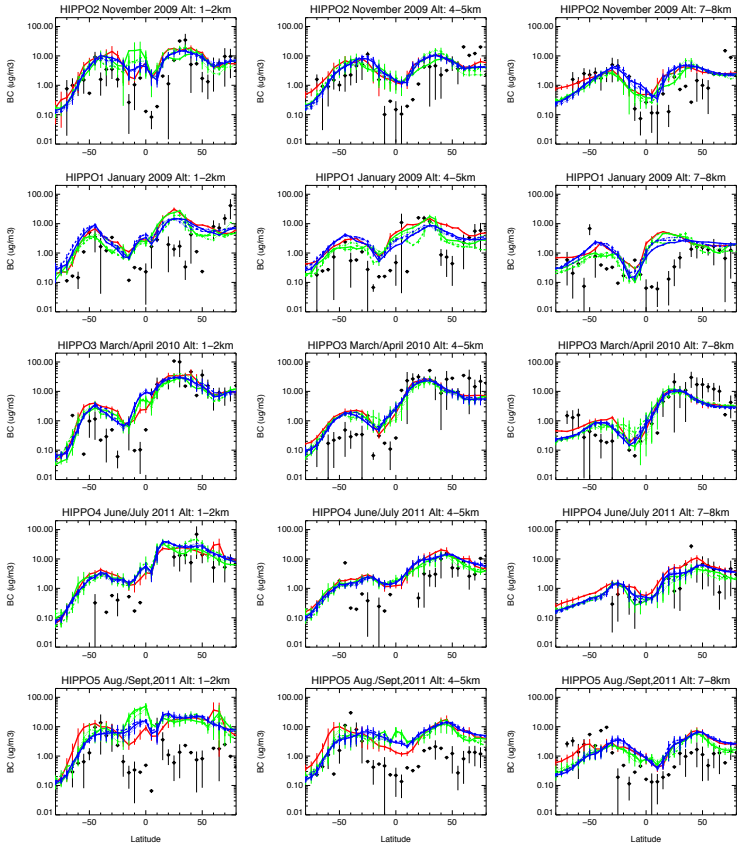


**Figure 11.** Black Carbon comparison between different HIPPO aircraft campaigns taken over the Pacific Ocean (black symbols) and results from the reference simulations REFC1SD (red), REFC1 (green), REFC2 (blue), averaged over different altitude intervals. The sampled aircraft profiles during different HIPPO campaigns were averaged over 5° latitude intervals along the flight path over the Pacific Ocean and compared to model output averaged over the same grid points, as done in Tilmes et al. (2015). The average profiles are averaged over three altitudes regions, 1-2 km, 4-5 km and 7-8 km.

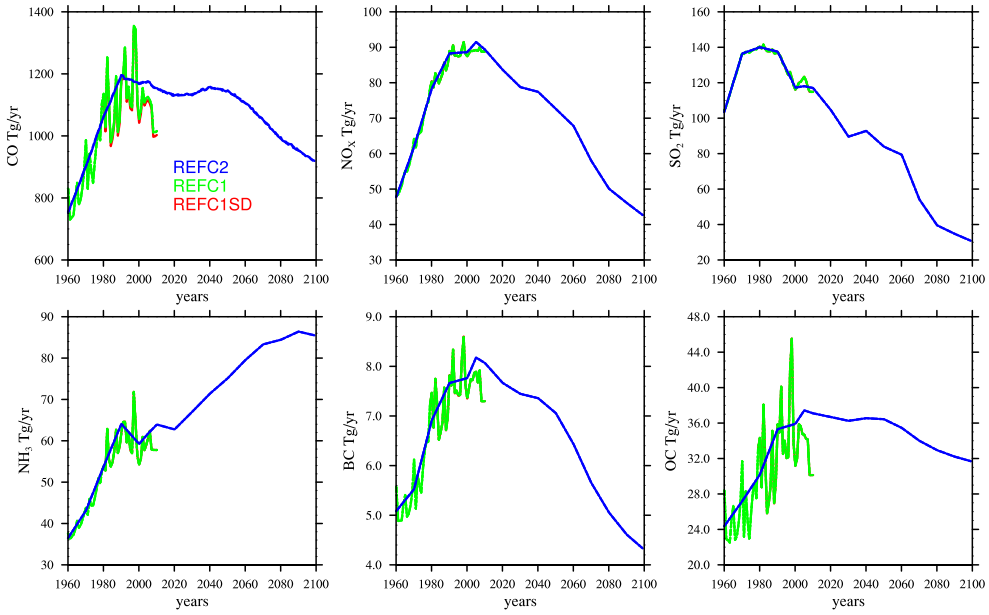


**Figure A1.** Selected surface emissions used for the different reference experiments.

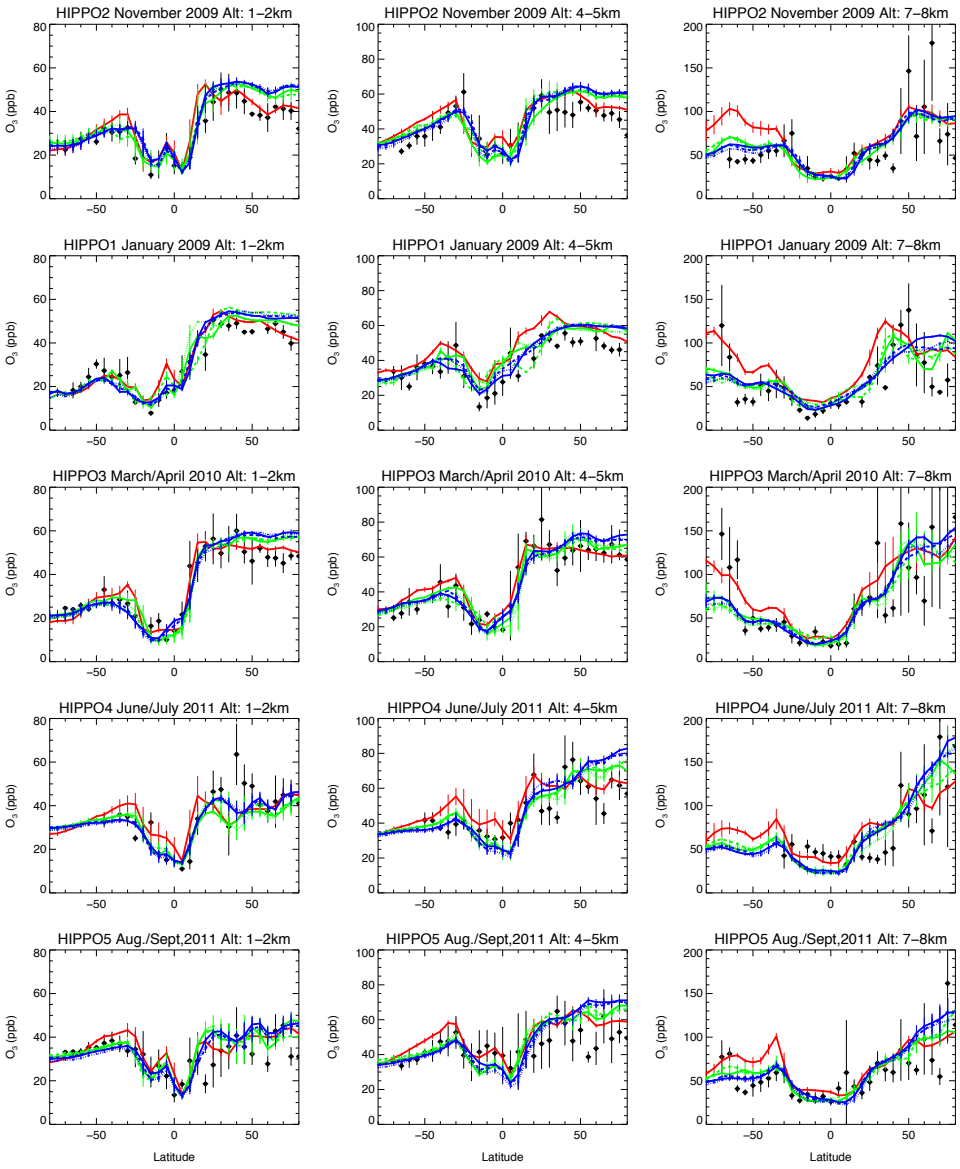


**Figure A2.** $O_3$ comparison between different HIPPO aircraft campaigns taken over the Pacific Ocean (black symbols) and results from the reference simulations REFC1SD (red), REFC1 (green), REFC2 (blue), averaged over different altitude intervals. The sampled aircraft profiles during different HIPPO campaigns were averaged over 5° latitude intervals along the flight path over the Pacific Ocean and compared to model output averaged over the same grid points, as done in Tilmes et al. (2015). The average profiles are averaged over three altitudes regions, 1-2 km, 4-5 km and 7-8 km.

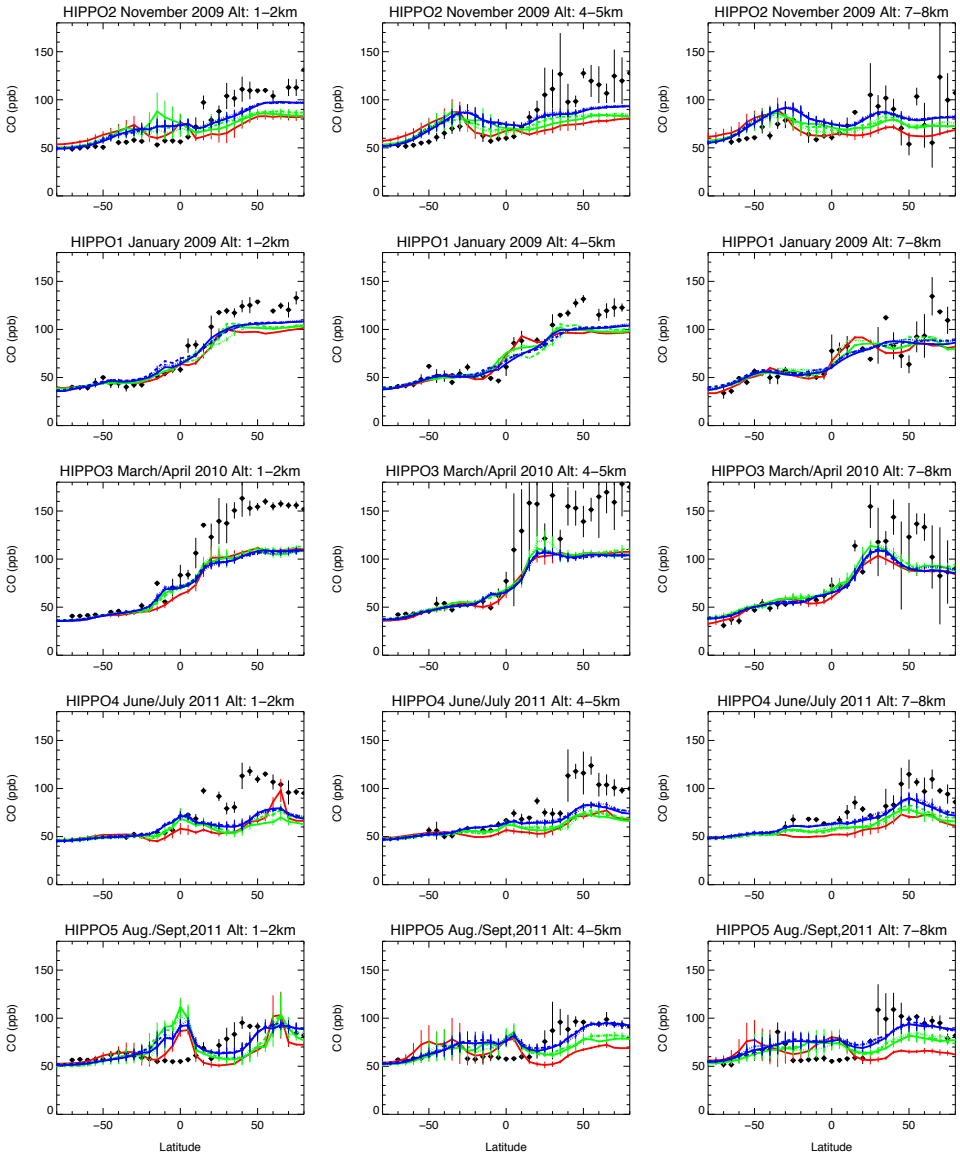


**Figure A3.** As Figure A2, but for Carbon Monoxide.

**Table 1.** Overview of global diagnostics for different experiments, averaged between 1995 and 2010. Lifetimes and burdens are calculated for the troposphere defined for regions where ozone is below 150 ppb.

| CESM1 CAM4chem | REFC1SD | REFC1.1 | REFC1.2 | REFC1.3 | REFC2.1 | REFC2.2 | REFC2.3 |
|---|---|---|---|---|---|---|---|
| Meteorology | MERRA | CAM4 | CAM4 | CAM4 | CAM4 | CAM4 | CAM4 |
| Vert. Res. | 56L | 26L | 26L | 26L | 26L | 26L | 26L |
| TS Global | 288.43 | 288.27 | 288.27 | 288.28 | 288.35 | 288.40 | 288.41 |
| TS Land | 282.37 | 282.10 | 282.12 | 282.17 | 282.23 | 282.20 | 282.23 |
| SWCF | -82.47 | -55.96 | -56.01 | -55.97 | -54.66 | -54.65 | -54.78 |
| $CH_4$ Burden (Tg) | 3991.3 | 4100.5 | 4103.8 | 4099.3 | 4101.4 | 4105.0 | 4103.1 |
| $CH_4$ Lifet. (yr) | 7.6 | 8.0 | 8.1 | 8.1 | 8.2 | 8.2 | 8.2 |
| $CH_3CCl_3$ Lifet. (yr) | 4.5 | 4.8 | 4.8 | 4.8 | 4.9 | 4.9 | 4.9 |
| CO Burden (Tg) | 289.6 | 303.6 | 305.3 | 305.7 | 315.4 | 316.7 | 315.3 |
| CO Emis. (Tg/yr) | 1114.8 | 1119.3 | 1126.5 | 1126.8 | 1170.1 | 1171.1 | 1169.9 |
| CO Dep. (Tg/yr) | 125.8 | 120.7 | 122.0 | 122.1 | 122.7 | 123.0 | 122.9 |
| CO Chem. Loss (Tg/yr) | 2264.1 | 2294.2 | 2295.3 | 2298.0 | 2348.4 | 2353.3 | 2345.5 |
| CO Lifet. (days) | 44.2 | 45.9 | 46.1 | 46.1 | 46.6 | 46.7 | 46.6 |
| $O_3$ Burden (Tg) | 332.5 | 326.9 | 326.5 | 326.4 | 327.8 | 327.2 | 327.0 |
| $O_3$ Dep. (Tg/yr) | 871.7 | 894.4 | 893.9 | 894.2 | 895.0 | 892.8 | 894.7 |
| $O_3$ Chem. Loss (Tg/yr) | 4256.0 | 4268.3 | 4250.6 | 4259.0 | 4287.6 | 4293.5 | 4278.9 |
| $O_3$ Chem. Prod. (Tg/yr) | 4693.8 | 4710.0 | 4706.5 | 4708.3 | 4747.2 | 4756.9 | 4744.1 |
| $O_3$ Net Chem.Change (Tg/yr) | 392.9 | 420.9 | 430.5 | 426.0 | 432.5 | 436.5 | 438.2 |
| $O_3$ STE (Tg/yr) | 478.8 | 473.4 | 463.4 | 468.2 | 462.5 | 456.4 | 456.5 |
| Isop. Emis. (Tg/yr) | 454.2 | 512.6 | 511.8 | 515.0 | 546.6 | 551.6 | 545.6 |
| Monoterp. Emis. (Tg/yr) | 138.9 | 150.0 | 150.0 | 150.3 | 155.4 | 156.4 | 155.0 |
| Methanol Emis. (Tg/yr) | 100.4 | 114.6 | 114.8 | 114.9 | 113.7 | 114.9 | 113.4 |
| Aceton Emis. (Tg/yr) | 41.6 | 44.3 | 44.3 | 44.3 | 47.8 | 48.1 | 47.7 |
| Lightning Prod. (TgN/yr) | 4.5 | 4.8 | 4.7 | 4.8 | 4.7 | 4.7 | 4.7 |
| Total optical depth | 0.107 | 0.119 | 0.119 | 0.119 | 0.118 | 0.118 | 0.118 |
| Dust optical depth | 0.041 | 0.043 | 0.043 | 0.043 | 0.040 | 0.041 | 0.040 |
| POM Burden (TgC) | 0.75 | 0.73 | 0.73 | 0.74 | 0.77 | 0.77 | 0.77 |
| POM Emis. (TgC/yr) | 48.38 | 47.99 | 48.38 | 48.38 | 51.23 | 51.23 | 51.23 |
| POM Lifet. (days) | 7.23 | 7.18 | 7.15 | 7.19 | 7.05 | 7.06 | 7.01 |
| SOA Burden (TgC) | 0.54 | 0.49 | 0.49 | 0.49 | 0.51 | 0.51 | 0.50 |
| SOA Chem. Prod. (TgC/yr) | 32.79 | 34.45 | 34.43 | 34.79 | 35.86 | 36.32 | 35.54 |
| SOA Lifet. (days) | 0.54 | 0.49 | 0.49 | 0.49 | 0.51 | 0.51 | 0.50 |
| BC Burden (TgC) | 0.12 | 0.12 | 0.12 | 0.12 | 0.12 | 0.12 | 0.12 |
| BC Emis. (TgC/yr) | 7.71 | 7.68 | 7.71 | 7.71 | 7.95 | 7.95 | 7.95 |
| BC Lifet. (days) | 7.44 | 7.48 | 7.46 | 7.49 | 5.88 | 5.89 | 5.86 |
| DUST Burden (TgC) | 43.87 | 45.04 | 45.03 | 45.20 | 42.60 | 42.75 | 42.31 |
| SALT Burden (TgC) | 6.02 | 10.88 | 10.88 | 10.87 | 11.14 | 11.10 | 11.11 |
| $SO_4$ Burden (TgS) | 0.45 | 0.49 | 0.49 | 0.49 | 0.51 | 0.51 | 0.51 |
| $SO_4$ Emis. (TgS/yr) | 0.25 | 0.25 | 0.25 | 0.25 | 0.25 | 0.25 | 0.25 |
| $SO_4$ Dry Dep. (TgS/yr) | 5.29 | 5.76 | 5.78 | 5.77 | 5.94 | 6.00 | 5.99 |
| $SO_4$ Wet Dep. (TgS/yr) | -49.93 | -46.36 | -46.28 | -46.30 | -46.36 | -46.42 | -46.49 |
| $SO_4$ Chem. Prod. (TgS/yr) | 10.35 | 10.81 | 10.83 | 10.82 | 10.98 | 11.02 | 11.02 |
| $SO_4$ AQ. Prod. (TgS/yr) | 44.95 | 41.41 | 41.34 | 41.35 | 41.44 | 41.53 | 41.58 |
| $SO_4$ Total Prod. (TgS/yr) | 55.30 | 52.23 | 52.17 | 52.18 | 52.42 | 52.55 | 52.60 |
| $SO_4$ Lifet. (days) | 2.97 | 3.41 | 3.42 | 3.41 | 3.52 | 3.54 | 3.53 |

**Table A1.** Chemical species in CAM4-chem, chemical formula, solver (either explict (E) or semi-implicit (~~S~~I)), lower boundary conditions (LBC), and wet and dry deposition of species.

| Num. | Species | Formula | Solver | Emis. | LBC | wet dep | dry dep |
|---|---|---|---|---|---|---|---|
| 1 | ALKO2 | (C5H11O2) | I | | | | |
| 2 | ALKOOH | (C5H12O2) | I | | | X | X |
| 3 | BENO2 | (C6H7O3) | I | | | | |
| 4 | BENOOH | (C6H8O3) | I | | | | |
| 5 | BENZENE | (C6H6) | I | X | | | |
| 6 | BIGALD | (C5H6O2) | I | X | | | |
| 7 | BIGALK | (C5H12) | I | X | | | |
| 8 | BIGENE | (C4H8) | I | X | | | |
| 9 | BR | (Br) | I | | | | |
| 10 | BRCL | (BrCl) | I | | | | |
| 11 | BRO | (BrO) | I | | | | |
| 12 | BRONO2 | (BrONO2) | I | | | X | |
| 13 | BRY | | E | | | | |
| 14 | C10H16 | | I | X | | | |
| 15 | C2H2 | | I | X | | | |
| 16 | C2H4 | | I | X | | | |
| 17 | C2H5O2 | | I | | | | |
| 18 | C2H5OH | | I | X | | X | X |
| 19 | C2H5OOH | | I | | | X | X |
| 20 | C2H6 | | I | X | | | |
| 21 | C3H6 | | I | X | | | |
| 22 | C3H7O2 | | I | | | | |
| 23 | C3H7OOH | | I | | | X | X |
| 24 | C3H8 | | I | X | | | |
| 25 | CCL4 | (CCl4) | E | | X | | |
| 26 | CF2CLBR | (CF2ClBr) | E | | X | | |
| 27 | CF3BR | (CF3Br) | E | | X | | |
| 28 | CFC11 | (CFCl3) | E | | X | | |
| 29 | CFC113 | (CCl2FCClF2) | E | | X | | |
| 30 | CFC114 | (CClF2CClF2) | E | | X | | |
| 31 | CFC115 | (CClF2CF3) | E | | X | | |
| 32 | CFC12 | (CF2Cl2) | E | | X | | |
| 33 | CH2BR2 | (CH2Br2) | E | | X | | |
| 34 | CH2O | | I | X | | X | X |
| 35 | CH3BR | (CH3Br) | E | | X | | |

**Table A1.** continued

| Num. | Species | Formula | Solver | Emis. | LBC | wet dep | dry dep |
|---|---|---|---|---|---|---|---|
| 36 | CH3CCL3 | (CH3CCl3) | E | | X | | |
| 37 | CH3CHO | | I | X | | X | X |
| 38 | CH3CL | (CH3Cl) | E | | X | | |
| 39 | CH3CN | | I | X | | X | X |
| 40 | CH3CO3 | | I | | | | |
| 41 | CH3COCH3 | | I | X | | X | X |
| 42 | CH3COCHO | | I | | | X | X |
| 43 | CH3COOH | | I | X | | | X |
| 44 | CH3COOOH | | I | | | X | X |
| 45 | CH3O2 | | I | | | | |
| 46 | CH3OH | | I | X | | X | X |
| 47 | CH3OOH | | I | | | X | X |
| 48 | CH4 | | E | | X | | |
| 49 | CHBR3 | (CHBr3) | E | | X | | |
| 50 | CL | (Cl) | I | | | | |
| 51 | CL2 | (Cl2) | I | | | | |
| 52 | CL2O2 | (Cl2O2) | I | | | | |
| 53 | CLO | (ClO) | I | | | | |
| 54 | CLONO2 | (ClONO2) | I | | | X | |
| 55 | CLY | | E | | | | |
| 56 | CO | | I | X | | | X |
| 57 | CO2 | | E | | X | | |
| 58 | CRESOL | (C7H8O) | I | | | | |
| 59 | DMS | (CH3SCH3) | I | X | | | |
| 60 | ENEO2 | (C4H9O3) | I | | | | |
| 61 | EO | (HOCH2CH2O) | I | | | | |
| 62 | EO2 | (HOCH2CH2O2) | I | | | | |
| 63 | EOOH | (HOCH2CH2OOH) | I | | | X | X |
| 64 | GLYALD | (HOCH2CHO) | I | | | X | X |
| 65 | GLYOXAL | (C2H2O2) | I | | | | |
| 66 | H | | I | | | | |
| 67 | H1202 | (CBr2F2) | E | | X | | |
| 68 | H2 | | I | | X | | |
| 69 | H2402 | (CBrF2CBrF2) | E | | X | | |
| 70 | H2O | | I | | | | |
| 71 | H2O2 | | I | | | X | X |
| 72 | HBR | (HBr) | I | | | X | |
| 73 | HCFC141B | (CH3CCl2F) | E | | X | | |
| 74 | HCFC142B | (CH3CClF2) | E | | X | | |

**Table A1.** continued

| Num. | Species | Formula | Solver | Emis. | LBC | wet dep | dry dep |
|---|---|---|---|---|---|---|---|
| 75 | HCFC22 | (CHF2Cl) | E | | X | | |
| 76 | HCL | (HCl) | I | | | X | |
| 77 | HCN | | I | X | | X | X |
| 78 | HCOOH | | I | X | | X | X |
| 79 | HNO3 | | I | | | X | X |
| 80 | HO2 | | I | | | | |
| 81 | HO2NO2 | | I | | | X | X |
| 82 | HOBR | (HOBr) | I | | | X | |
| 83 | HOCH2OO | | I | | | | |
| 84 | HOCL | (HOCl) | I | | | X | |
| 85 | HYAC | (CH3COCH2OH) | I | | | X | X |
| 86 | HYDRALD | (HOCH2CCH3CHCHO) | I | | | X | X |
| 87 | ISOP | (C5H8) | I | X | | | |
| 88 | ISOPNO3 | (CH2CHCCH3OOCH2ONO2) | I | | | X | |
| 89 | ISOPO2 | (HOCH2COOCH3CHCH2) | I | | | | |
| 90 | ISOPOOH | (HOCH2COOHCH3CHCH2) | I | | | X | X |
| 91 | MACR | (CH2CCH3CHO) | I | | | X | |
| 92 | MACRO2 | (CH3COCHO2CH2OH) | I | | | | |
| 93 | MACROOH | (CH3COCHOOHCH2OH) | I | | | X | X |
| 94 | MCO3 | (CH2CCH3CO3) | I | | | | |
| 95 | MEK | (C4H8O) | I | X | | | |
| 96 | MEKO2 | (C4H7O3) | I | | | | |
| 97 | MEKOOH | (C4H8O3) | I | | | X | X |
| 98 | MPAN | (CH2CCH3CO3NO2) | I | | | | X |
| 99 | MVK | (CH2CHCOCH3) | I | | | X | |
| 100 | N | | I | | | | |
| 101 | N2O | | E | | X | | |
| 102 | N2O5 | | I | | | | |
| 103 | NH3 | | I | X | | X | X |
| 104 | NO | | I | X | | | X |
| 105 | NO2 | | I | | | | X |
| 106 | NO3 | | I | | | | |
| 107 | O | | I | | | | |
| 108 | O1D | (O) | I | | | | |
| 109 | O3 | | I | | | | X |
| 110 | OCLO | (OClO) | I | | | | |
| 111 | OH | | I | | | | |
| 112 | ONIT | (CH3COCH2ONO2) | I | | | X | X |

**Table A1.** continued

| Num. | Species | Formula | Solver | Emis. | LBC | wet dep | dry dep |
|---|---|---|---|---|---|---|---|
| 113 | ONITR | (CH2CCH3CHONO2CH2OH) | I | | | X | X |
| 114 | PAN | (CH3CO3NO2) | I | | | | X |
| 115 | PO2 | (C3H6OHO2) | I | | | | |
| 116 | POOH | (C3H6OHOOH) | I | | | X | X |
| 117 | RO2 | (CH3COCH2O2) | I | | | | |
| 118 | ROOH | (CH3COCH2OOH) | I | | | X | X |
| 119 | SF6 | | E | | X | | |
| 120 | SO2 | | I | X | | X | X |
| 121 | SOGB | (C6H7O3) | I | | | X | X |
| 122 | SOGI | (CH3C4H9O4) | I | | | X | X |
| 123 | SOGM | (C10H16O4) | I | | | X | X |
| 124 | SOGT | (C7H9O3) | I | | | X | X |
| 125 | SOGX | (C8H11O3) | I | | | X | X |
| 126 | TERPO2 | (C10H17O3) | I | | | | |
| 127 | TERPOOH | (C10H18O3) | I | | | X | X |
| 128 | TOLO2 | (C7H9O5) | I | | | | |
| 129 | TOLOOH | (C7H10O5) | I | | | X | X |
| 130 | TOLUENE | (C7H8) | I | X | | | |
| 131 | XO2 | (HOCH2COOCH3CHOHCHO) | I | | | | |
| 132 | XOH | (C7H10O6) | I | | | | |
| 133 | XOOH | (HOCH2COOHCH3CHOHCHO) | I | | | X | X |
| 134 | XYLENE | (C8H10) | I | | | | |
| 135 | XYLO2 | (C8H11O3) | I | | | | |
| 136 | XYLOOH | (C8H12O3) | I | | | | |

**Table A1.** continued

| Num. | Aerosols | Formula | Solver | Emis. | LBC | wet dep | dry dep |
|---|---|---|---|---|---|---|---|
| 1 | CB1 | (C), hydrophobic BC | I | X | | X | |
| 2 | CB2 | (C) hydrophilic BC | I | X | | X | |
| 3 | NH4 | | I | | | | NH4 |
| 4 | NH4NO3 | | I | | | | X |
| 5 | OC1 | (C), hydrophobic OC | I | X | | | X |
| 6 | OC2 | (C) hydrophilic OC | I | X | | | X |
| 7 | DST01 | (AlSiO5) | I | | | | |
| 8 | DST02 | (AlSiO5) | I | | | | |
| 9 | DST03 | (AlSiO5) | I | | | | |
| 10 | DST04 | (AlSiO5) | I | | | | |
| 11 | SO4 | | I | | | | X |
| 12 | SOAB | (C6H7O3) | I | | | | X |
| 13 | SOAI | (CH3C4H9O4) | I | | | | X |
| 14 | SOAM | (C10H16O4) | I | | | | X |
| 15 | SOAT | (C7H9O3) | I | | | | X |
| 16 | SOAX | (C8H11O3) | I | | | | X |
| 17 | SSLT01 | (NaCl) | I | | | | |
| 18 | SSLT02 | (NaCl) | I | | | | |
| 19 | SSLT03 | (NaCl) | I | | | | |
| 20 | SSLT04 | (NaCl) | I | | | | |
| Num. | Artificial Tracers | Formula | Solver | Emis. | LBC | wet dep | dry dep |
| 1 | $AOA_{NH}$ | (H) | E | | | | |
| 2 | $CO_{25}$ | (CO) | E | X | | | |
| 3 | $CO_{50}$ | (CO) | E | X | | | |
| 4 | E90 | (CO) | E | X | | | |
| 5 | $E90_{NH}$ | (CO) | E | X | | | |
| 6 | $E90_{SH}$ | (CO) | E | X | | | |
| 7 | $NH_5$ | (H) | E | | | | |
| 8 | $NH_{50}$ | (H) | E | | | | |
| 9 | $NH_{50}W$ | (H) | E | | | X | |
| 10 | O3S | (O3) | E | | | | |
| 11 | SF6em | (SF6) | E | X | | | |
| 12 | SO2t | (SO2) | E | | | X | |
| 13 | $ST80_25$ | (H) | E | | | | |

**Table A2.** Chemical reactions in CAM4-chem

| Photolysis |
|---|
| O2 + hv → 2*O |
| O3 + hv → O1D + O2 |
| O3 + hv → O + O2 |
| N2O + hv → O1D + N2 |
| NO + hv → N + O |
| NO2 + hv → NO + O |
| N2O5 + hv → NO2 + NO3 |
| N2O5 + hv → NO + O + NO3 |
| HNO3 + hv → NO2 + OH |
| NO3 + hv → NO2 + O |
| NO3 + hv → NO + O2 |
| HO2NO2 + hv → OH + NO3 |
| HO2NO2 + hv → NO2 + HO2 |
| CH3OOH + hv → CH2O + H + OH |
| CH2O + hv → CO + 2*H |
| CH2O + hv → CO + H2 |
| H2O + hv → OH + H |
| H2O + hv → H2 + O1D |
| H2O + hv → 2*H + O |
| H2O2 + hv → 2*OH |
| CL2 + hv → 2*CL |
| CLO + hv → CL + O |
| OCLO + hv → O + CLO |
| CL2O2 + hv → 2*CL |
| HOCL + hv → OH + CL |
| HCL + hv → H + CL |
| CLONO2 + hv → CL + NO3 |
| CLONO2 + hv → CLO + NO2 |
| BRCL + hv → BR + CL |
| BRO + hv → BR + O |
| HOBR + hv → BR + OH |
| HBR + hv → BR + H |
| BRONO2 + hv → BR + NO3 |
| BRONO2 + hv → BRO + NO2 |
| CH3CL + hv → CL + CH3O2 |
| CCL4 + hv → 4*CL |
| CH3CCL3 + hv → 3*CL |
| CFC11 + hv → 3*CL |
| CFC12 + hv → 2*CL |
| CFC113 + hv → 3*CL |
| HCFC22 + hv → CL |
| CFC114 + hv → 2*CL |
| CFC115 + hv → CL |

**Table A2.** continued

| Photolysis |
|---|
| HCFC141B + hv → 2*CL |
| HCFC142B + hv → CL |
| CH3BR + hv → BR + CH3O2 |
| CF3BR + hv → BR |
| H1202 + hv → 2*BR |
| H2402 + hv → 2*BR |
| CF2CLBR + hv → BR + CL |
| CHBR3 + hv → 3*BR |
| CH2BR2 + hv → 2*BR |
| CO2 + hv → CO + O |
| CH4 + hv → H + CH3O2 |
| CH4 + hv → 1.44*H2 + 0.18*CH2O + 0.18*O + 0.33*OH + 0.33*H + 0.44*CO2 + 0.38*CO + 0.05*H2O |
| CH3CHO + hv → CH3O2 + CO + HO2 |
| POOH + hv → CH3CHO + CH2O + HO2 + OH |
| CH3COOOH + hv → CH3O2 + OH + CO2 |
| PAN + hv → .6*CH3CO3 + .6*NO2 + .4*CH3O2 + .4*NO3 + .4*CO2 |
| MPAN + hv → MCO3 + NO2 |
| MACR + hv → 1.34*HO2 + .66*MCO3 + 1.34*CH2O + 1.34*CH3CO3 |
| MACR + hv → .66*HO2 + 1.34*CO |
| MVK + hv → .7*C3H6 + .7*CO + .3*CH3O2 + .3*CH3CO3 |
| C2H5OOH + hv → CH3CHO + HO2 + OH |
| EOOH + hv → EO + OH |
| C3H7OOH + hv → 0.82*CH3COCH3 + OH + HO2 |
| ROOH + hv → CH3CO3 + CH2O + OH |
| CH3COCH3 + hv → CH3CO3 + CH3O2 |
| CH3COCHO + hv → CH3CO3 + CO + HO2 |
| XOOH + hv → OH |
| ONITR + hv → HO2 + CO + NO2 + CH2O |
| ISOPOOH + hv → .402*MVK + .288*MACR + .69*CH2O + HO2 |
| HYAC + hv → CH3CO3 + HO2 + CH2O |
| GLYALD + hv → 2*HO2 + CO + CH2O |
| MEK + hv → CH3CO3 + C2H5O2 |
| BIGALD + hv → .45*CO + .13*GLYOXAL + .56*HO2 + .13*CH3CO3 + .18*CH3COCHO |
| GLYOXAL + hv → 2*CO + 2*HO2 |
| ALKOOH + hv → .4*CH3CHO + .1*CH2O + .25*CH3COCH3 + .9*HO2 + .8*MEK + OH |
| MEKOOH + hv → OH + CH3CO3 + CH3CHO |
| TOLOOH + hv → OH + .45*GLYOXAL + .45*CH3COCHO + .9*BIGALD |
| TERPOOH + hv → OH + .1*CH3COCH3 + HO2 + MVK + MACR |
| SF6 + hv → sink |
| SF6em + hv → sink |

**Table A2.** continued

| Odd-Oxygen Reactions | Rate |
|---|---|
| O + O2 + M → O3 + M | 6.E-34*(300/T)**2.4 |
| O + O3 → 2*O2 | 8.00E-12*exp( -2060./t) |
| O + O + M → O2 + M | 2.76E-34*exp( 720./t) |
| **Odd-Oxygen Reactions (O1D only)** | |
| O1D + N2 → O + N2 | 2.15E-11*exp( 110./t) |
| O1D + O2 → O + O2 | 3.30E-11*exp( 55./t) |
| O1D + H2O → 2*OH | 1.63E-10*exp( 60./t) |
| O1D + N2O → 2*NO | 7.25E-11*exp( 20./t) |
| O1D + N2O → N2 + O2 | 4.63E-11*exp( 20./t) |
| O1D + O3 → O2 + O2 | 1.20E-10 |
| O1D + CFC11 → 3*CL | 2.02E-10 |
| O1D + CFC12 → 2*CL | 1.20E-10 |
| O1D + CFC113 → 3*CL | 1.50E-10 |
| O1D + CFC114 → 2*CL | 9.75E-11 |
| O1D + CFC115 → CL | 1.50E-11 |
| O1D + HCFC22 → CL | 7.20E-11 |
| O1D + HCFC141B → 2*CL | 1.79E-10 |
| O1D + HCFC142B → CL | 1.63E-10 |
| O1D + CCL4 → 4*CL | 2.84E-10 |
| O1D + CH3BR → BR | 1.67E-10 |
| O1D + CF2CLBR → CL + BR | 9.60E-11 |
| O1D + CF3BR → BR | 4.10E-11 |
| O1D + H1202 → 2*BR | 1.01E-10 |
| O1D + H2402 → 2*BR | 1.20E-10 |
| O1D + CHBR3 → 3*BR | 4.49E-10 |
| O1D + CH2BR2 → 2*BR | 2.57E-10 |
| O1D + CH4 → CH3O2 + OH | 1.31E-10 |
| O1D + CH4 → CH2O + H + HO2 | 3.50E-11 |
| O1D + CH4 → CH2O + H2 | 9.00E-12 |
| O1D + H2 → H + OH | 1.20E-10 |
| O1D + HCL → CL + OH | 1.50E-10 |
| O1D + HBR → BR + OH | 1.20E-10 |
| O1D + HCN → OH | 7.70E-11*exp( 100./t) |
| **Odd Hydrogen Reactions** | |
| H + O2 + M → HO2 + M | ko=4.40E-32*(300/t)**1.30<br>ki=7.50E-11*(300/t)**-0.20<br>f=0.60 |
| H + O3 → OH + O2 | 1.40E-10*exp( -470./t) |
| H + HO2 → 2*OH | 7.20E-11 |
| H + HO2 → H2 + O2 | 6.90E-12 |
| H + HO2 → H2O + O | 1.60E-12 |
| OH + O → H + O2 | 1.80E-11*exp( 180./t) |
| OH + O3 → HO2 + O2 | 1.70E-12*exp( -940./t) |
| OH + HO2 → H2O + O2 | 4.80E-11*exp( 250./t) |
| OH + OH → H2O + O | 1.80E-12 |
| OH + OH + M → H2O2 + M | ko=6.90E-31*(300/t)**1.00<br>ki=2.60E-11<br>f=0.60 |

**Table A2.** continued

| | |
|---|---|
| Odd Hydrogen Reactions | |
| OH + H2 → H2O + H | 2.80E-12*exp( -1800./t) |
| OH + H2O2 → H2O + HO2 | 1.80E-12 |
| H2 + O → OH + H | 1.60E-11*exp( -4570./t) |
| HO2 + O → OH + O2 | 3.00E-11*exp( 200./t) |
| HO2 + O3 → OH + 2*O2 | 1.00E-14*exp( -490./t) |
| HO2 + HO2 → H2O2 + O2 | 3.0E-13*exp(460/t)<br>+ 2.1E-33 * [M] * exp (920/t))<br>* (1 + 1.4E-21 * [H2O] exp (2200/t)) |
| H2O2 + O → OH + HO2 | 1.40E-12*exp( -2000./t) |
| HCN + OH + M → HO2 + M | ko=4.28E-33<br>ki=9.30E-15*(300/t)**-4.42<br>f=0.80 |
| CH3CN + OH → HO2 | 7.80E-13*exp( -1050./t) |
| Odd Nitrogen Reactions | |
| N + O2 → NO + O | 1.50E-11*exp( -3600./t) |
| N + NO → N2 + O | 2.10E-11*exp( 100./t) |
| N + NO2 → N2O + O | 2.90E-12*exp( 220./t) |
| N + NO2 → 2*NO | 1.45E-12*exp( 220./t) |
| N + NO2 → N2 + O2 | 1.45E-12*exp( 220./t) |
| NO + O + M → NO2 + M | ko=9.00E-32*(300/t)**1.50<br>ki=3.00E-11<br>f=0.60 |
| NO + HO2 → NO2 + OH | 3.30E-12*exp( 270./t) |
| NO + O3 → NO2 + O2 | 3.00E-12*exp( -1500./t) |
| NO2 + O → NO + O2 | 5.10E-12*exp( 210./t) |
| NO2 + O + M → NO3 + M | ko=2.50E-31*(300/t)**1.80<br>ki=2.20E-11*(300/t)**0.70<br>f=0.60 |
| NO2 + O3 → NO3 + O2 | 1.20E-13*exp( -2450./t) |
| NO2 + NO3 + M → N2O5 + M | ko=2.00E-30*(300/t)**4.40<br>ki=1.40E-12*(300/t)**0.70<br>f=0.60 |
| N2O5 + M → NO2 + NO3 + M | k(NO2 + NO3 + M)<br>* 3.704E26 * exp(-11000./t) |
| NO2 + OH + M → HNO3 + M | ko=1.80E-30*(300/t)**3.00<br>ki=2.80E-11<br>f=0.60 |
| HNO3 + OH → NO3 + H2O | k0 + k3[M]/(1 + k3[M]/k2)<br>k0 = 2.4E-14*exp(460/t)<br>k2 = 2.7E-17*exp(2199/t)<br>k3 = 6.5E-34*exp(1335/t) |
| NO3 + NO → 2*NO2 | 1.50E-11*exp( 170./t) |
| NO3 + O → NO2 + O2 | 1.00E-11 |
| NO3 + OH → HO2 + NO2 | 2.20E-11 |
| NO3 + HO2 → OH + NO2 + O2 | 3.50E-12 |
| NO2 + HO2 + M → HO2NO2 + M | ko=2.00E-31*(300/t)**3.40<br>ki=2.90E-12*(300/t)**1.10<br>f=0.60 |
| HO2NO2 + OH → H2O + NO2 + O2 | 1.30E-12*exp( 380./t) |
| HO2NO2 + M → HO2 + NO2 + M | k(NO2+HO2+M)<br>* exp(-10900/t)/2.1E-27 |

**Table A2.** continued

| Odd Chlorine Reactions | |
|---|---|
| CL + O3 → CLO + O2 | 2.30E-11*exp( -200./t) |
| CL + H2 → HCL + H | 3.05E-11*exp( -2270./t) |
| CL + H2O2 → HCL + HO2 | 1.10E-11*exp( -980./t) |
| CL + HO2 → HCL + O2 | 1.40E-11*exp( 270./t) |
| CL + HO2 → OH + CLO | 3.60E-11*exp( -375./t) |
| CL + CH2O → HCL + HO2 + CO | 8.10E-11*exp( -30./t) |
| CL + CH4 → CH3O2 + HCL | 7.30E-12*exp( -1280./t) |
| CLO + O → CL + O2 | 2.80E-11*exp( 85./t) |
| CLO + OH → CL + HO2 | 7.40E-12*exp( 270./t) |
| CLO + OH → HCL + O2 | 6.00E-13*exp( 230./t) |
| CLO + HO2 → O2 + HOCL | 2.60E-12*exp( 290./t) |
| CLO + CH3O2 → CL + HO2 + CH2O | 3.30E-12*exp( -115./t) |
| CLO + NO → NO2 + CL | 6.40E-12*exp( 290./t) |
| CLO + NO2 + M → CLONO2 + M | ko=1.80E-31*(300/t)**3.40<br>ki=1.50E-11*(300/t)**1.90<br>f=0.60 |
| CLO + CLO → 2*CL + O2 | 3.00E-11*exp( -2450./t) |
| CLO + CLO → CL2 + O2 | 1.00E-12*exp( -1590./t) |
| CLO + CLO → CL + OCLO | 3.50E-13*exp( -1370./t) |
| CLO + CLO + M → CL2O2 + M | ko=1.60E-32*(300/t)**4.50<br>ki=3.00E-12*(300/t)**2.00<br>f=0.60 |
| CL2O2 + M → CLO + CLO + M | k(CLO+CLO+M) / (1.72E-27*exp(8649./t)) |
| HCL + OH → H2O + CL | 1.80E-12*exp( -250./t) |
| HCL + O → CL + OH | 1.00E-11*exp( -3300./t) |
| HOCL + O → CLO + OH | 1.70E-13 |
| HOCL + CL → HCL + CLO | 3.40E-12*exp( -130./t) |
| HOCL + OH → H2O + CLO | 3.00E-12*exp( -500./t) |
| CLONO2 + O → CLO + NO3 | 3.60E-12*exp( -840./t) |
| CLONO2 + OH → HOCL + NO3 | 1.20E-12*exp( -330./t) |
| CLONO2 + CL → CL2 + NO3 | 6.50E-12*exp( 135./t) |
| **Odd Bromine Reactions** | |
| BR + O3 → BRO + O2 | 1.60E-11*exp( -780./t) |
| BR + HO2 → HBR + O2 | 4.80E-12*exp( -310./t) |
| BR + CH2O → HBR + HO2 + CO | 1.70E-11*exp( -800./t) |
| BRO + O → BR + O2 | 1.90E-11*exp( 230./t) |
| BRO + OH → BR + HO2 | 1.70E-11*exp( 250./t) |
| BRO + HO2 → HOBR + O2 | 4.50E-12*exp( 460./t) |
| BRO + NO → BR + NO2 | 8.80E-12*exp( 260./t) |
| BRO + NO2 + M → BRONO2 + M | ko=5.20E-31*(300/t)**3.20<br>ki=6.90E-12*(300/t)**2.90<br>f=0.60 |
| BRO + CLO → BR + OCLO | 9.50E-13*exp( 550./t) |
| BRO + CLO → BR + CL + O2 | 2.30E-12*exp( 260./t) |
| BRO + CLO → BRCL + O2 | 4.10E-13*exp( 290./t) |
| BRO + BRO → 2*BR + O2 | 1.50E-12*exp( 230./t) |
| HBR + OH → BR + H2O | 5.50E-12*exp( 200./t) |
| HBR + O → BR + OH | 5.80E-12*exp( -1500./t) |
| HOBR + O → BRO + OH | 1.20E-10*exp( -430./t) |
| BRONO2 + O → BRO + NO3 | 1.90E-11*exp( 215./t) |

**Table A2.** continued

| Organic Halogens Reactions with Cl, OH | Rate |
|---|---|
| CH3CL + CL → HO2 + CO + 2*HCL | 2.17E-11*exp( -1130./t) |
| CH3CL + OH → CL + H2O + HO2 | 2.40E-12*exp( -1250./t) |
| CH3CCL3 + OH → H2O + 3*CL | 1.64E-12*exp( -1520./t) |
| HCFC22 + OH → H2O + CL | 1.05E-12*exp( -1600./t) |
| CH3BR + OH → BR + H2O + HO2 | 2.35E-12*exp( -1300./t) |
| CH3BR + CL → HCL + HO2 + BR | 1.40E-11*exp( -1030./t) |
| HCFC141B + OH → 2*CL | 1.25E-12*exp( -1600./t) |
| HCFC142B + OH → CL | 1.30E-12*exp( -1770./t) |
| CH2BR2 + OH → 2*BR + H2O | 2.00E-12*exp( -840./t) |
| CHBR3 + OH → 3*BR | 1.35E-12*exp( -600./t) |
| CH2BR2 + CL → 2*BR + HCL | 6.30E-12*exp( -800./t) |
| CHBR3 + CL → 3*BR + HCL | 4.85E-12*exp( -850./t) |
| C-1 Degradation (Methane, CO, CH2O and derivatives) | |
| CH4 + OH → CH3O2 + H2O | 2.45E-12*exp( -1775./t) |
| CO + OH → CO2 + H | ki = 2.1E09 * (t/300)**6.1<br>ko = 1.5E-13 * (t/300)**0.6<br>rate=ko/(1+ko/(ki/M))<br>*0.6**(1/(1+log10(ko/(ki/M)**2))) |
| CO + OH + M → CO2 + HO2 + M | ko=5.90E-33*(300/t)**1.40<br>ki=1.10E-12*(300/t)**-1.30<br>f=0.60 |
| CH2O + NO3 → CO + HO2 + HNO3 | 6.00E-13*exp( -2058./t) |
| CH2O + OH → CO + H2O + H | 5.50E-12*exp( 125./t) |
| CH2O + O → HO2 + OH + CO | 3.40E-11*exp( -1600./t) |
| CH2O + HO2 → HOCH2OO | 9.70E-15*exp( 625./t) |
| CH3O2 + NO → CH2O + NO2 + HO2 | 2.80E-12*exp( 300./t) |
| CH3O2 + HO2 → CH3OOH + O2 | 4.10E-13*exp( 750./t) |
| CH3O2 + CH3O2 → 2*CH2O + 2*HO2 | 5.00E-13*exp( -424./t) |
| CH3O2 + CH3O2 → CH2O + CH3OH | 1.90E-14*exp( 706./t) |
| CH3OH + OH → HO2 + CH2O | 2.90E-12*exp( -345./t) |
| CH3OOH + OH → .7*CH3O2 + .3*OH + .3*CH2O + H2O | 3.80E-12*exp( 200./t) |
| HCOOH + OH → HO2 + CO2 + H2O | 4.50E-13 |
| HOCH2OO → CH2O + HO2 | 2.40E+12*exp( -7000./t) |
| HOCH2OO + NO → HCOOH + NO2 + HO2 | 2.60E-12*exp( 265./t) |
| HOCH2OO + HO2 → HCOOH | 7.50E-13*exp( 700./t) |
| C-2 Degradation | |
| C2H2 + CL + M → CL + M | ko=5.20E-30*(300/t)**2.40<br>ki=2.20E-10*(300/t)**0.70<br>f=0.60 |
| C2H4 + CL + M → CL + M | ko=1.60E-29*(300/t)**3.30<br>ki=3.10E-10*(300/t)<br>f=0.60 |
| C2H6 + CL → HCL + C2H5O2 | 7.20E-11*exp( -70./t) |
| C2H2 + OH + M → .65*GLYOXAL + .65*OH + .35*HCOOH + .35*HO2 + .35*CO + M | ko=5.50E-30<br>ki=8.30E-13*(300/t)**-2.00<br>f=0.60 |
| C2H6 + OH → C2H5O2 + H2O | 7.66E-12*exp( -1020./t) |
| C2H4 + OH + M → EO2 + M | ko=8.60E-29*(300/t)**3.10<br>ki=9.00E-12*(300/t)**0.85<br>f=0.48 |

**Table A2.** continued

| C-2 Degradation | |
|---|---|
| EO2 + NO → 0.5*CH2O + 0.25*HO2 + 0.75*EO + NO2 | 4.20E-12*exp( 180./t) |
| EO2 + HO2 → EOOH | 7.50E-13*exp( 700./t) |
| EO + O2 → GLYALD + HO2 | 1.00E-14 |
| EO → 2*CH2O + HO2 | 1.60E+11*exp( -4150./t) |
| C2H4 + O3 → CH2O + .12*HO2 + .5*CO + .12*OH + .5*HCOOH | 1.20E-14*exp( -2630./t) |
| CH3COOH + OH → CH3O2 + CO2 + H2O | 7.00E-13 |
| C2H5O2 + NO → CH3CHO + HO2 + NO2 | 2.60E-12*exp( 365./t) |
| C2H5O2 + HO2 → C2H5OOH + O2 | 7.50E-13*exp( 700./t) |
| C2H5O2 + CH3O2 → .7*CH2O + .8*CH3CHO + HO2 + .3*CH3OH + .2*C2H5OH | 2.00E-13 |
| C2H5O2 + C2H5O2 → 1.6*CH3CHO + 1.2*HO2 + .4*C2H5OH | 6.80E-14 |
| C2H5OOH + OH → .5*C2H5O2 + .5*CH3CHO + .5*OH | 3.80E-12*exp( 200./t) |
| CH3CHO + OH → CH3CO3 + H2O | 4.63E-12*exp( 350./t) |
| CH3CHO + NO3 → CH3CO3 + HNO3 | 1.40E-12*exp( -1900./t) |
| CH3CO3 + NO → CH3O2 + CO2 + NO2 | 8.10E-12*exp( 270./t) |
| CH3CO3 + NO2 + M → PAN + M | ko=9.70E-29*(300/t)**5.60<br>ki=9.30E-12*(300/t)**1.50<br>f=0.60 |
| CH3CO3 + HO2 → .75*CH3COOOH + .25*CH3COOH + .25*O3 | 4.30E-13*exp( 1040./t) |
| CH3CO3 + CH3O2 → .9*CH3O2 + CH2O + .9*HO2 + .9*CO2 + .1*CH3COOH | 2.00E-12*exp( 500./t) |
| CH3CO3 + CH3CO3 → 2*CH3O2 + 2*CO2 | 2.50E-12*exp( 500./t) |
| CH3COOOH + OH → .5*CH3CO3 + .5*CH2O + .5*CO2 + H2O | 1.00E-12 |
| GLYALD + OH → HO2 + .2*GLYOXAL + .8*CH2O + .8*CO2 | 1.00E-11 |
| GLYOXAL + OH → HO2 + CO + CO2 | 1.15E-11 |
| C2H5OH + OH → HO2 + CH3CHO | 6.90E-12*exp( -230./t) |
| PAN + M → CH3CO3 + NO2 + M | k(CH3CO3+NO2+M)<br>*1.111E28 * exp(-14000/t) |
| PAN + OH → CH2O + NO3 | 4.00E-14 |

| C-3 Degradation | Rate |
|---|---|
| C3H6 + OH + M → PO2 + M | ko=8.00E-27*(300/t)**3.50<br>ki=3.00E-11<br>f=0.50 |
| C3H6 + O3 → .54*CH2O + .19*HO2 + .33*OH + .08*CH4 + .56*CO + .5*CH3CHO + .31*CH3O2 + .25*CH3COOH | 6.50E-15*exp( -1900./t) |
| C3H6 + NO3 → ONIT | 4.60E-13*exp( -1156./t) |
| C3H7O2 + NO → .82*CH3COCH3 + NO2 + HO2 + .27*CH3CHO | 4.20E-12*exp( 180./t) |
| C3H7O2 + HO2 → C3H7OOH + O2 | 7.50E-13*exp( 700./t) |
| C3H7O2 + CH3O2 → CH2O + HO2 + .82*CH3COCH3 | 3.75E-13*exp( -40./t) |
| C3H7OOH + OH → H2O + C3H7O2 | 3.80E-12*exp( 200./t) |
| C3H8 + OH → C3H7O2 + H2O | 8.70E-12*exp( -615./t) |
| PO2 + NO → CH3CHO + CH2O + HO2 + NO2 | 4.20E-12*exp( 180./t) |
| PO2 + HO2 → POOH + O2 | 7.50E-13*exp( 700./t) |
| POOH + OH → .5*PO2 + .5*OH + .5*HYAC + H2O | 3.80E-12*exp( 200./t) |
| CH3COCH3 + OH → RO2 + H2O | 3.82E-11*exp(-2000/t) + .33E-13 |
| RO2 + NO → CH3CO3 + CH2O + NO2 | 2.90E-12*exp( 300./t) |
| RO2 + HO2 → ROOH + O2 | 8.60E-13*exp( 700./t) |
| RO2 + CH3O2 → .3*CH3CO3 + .8*CH2O + .3*HO2 + .2*HYAC + .5*CH3COCHO + .5*CH3OH | 7.10E-13*exp( 500./t) |

**Table A2.** continued

| C-3 Degradation | Rate |
|---|---|
| ROOH + OH → RO2 + H2O | 3.80E-12*exp( 200./t) |
| HYAC + OH → CH3COCHO + HO2 | 3.00E-12 |
| CH3COCHO + OH → CH3CO3 + CO + H2O | 8.40E-13*exp( 830./t) |
| CH3COCHO + NO3 → HNO3 + CO + CH3CO3 | 1.40E-12*exp( -1860./t) |
| ONIT + OH → NO2 + CH3COCHO | 6.80E-13 |
| **C-4 Degradation** | |
| BIGENE + OH → ENEO2 | 5.40E-11 |
| ENEO2 + NO → CH3CHO + .5*CH2O + .5*CH3COCH3 + HO2 + NO2 | 4.20E-12*exp( 180./t) |
| MVK + OH → MACRO2 | 4.13E-12*exp( 452./t) |
| MVK + O3 → .8*CH2O + .95*CH3COCHO + .08*OH + .2*O3 + .06*HO2 + .05*CO + .04*CH3CHO | 7.52E-16*exp( -1521./t) |
| MEK + OH → MEKO2 | 2.30E-12*exp( -170./t) |
| MEKO2 + NO → CH3CO3 + CH3CHO + NO2 | 4.20E-12*exp( 180./t) |
| MEKO2 + HO2 → MEKOOH | 7.50E-13*exp( 700./t) |
| MEKOOH + OH → MEKO2 | 3.80E-12*exp( 200./t) |
| MACR + OH → .5*MACRO2 + .5*H2O + .5*MCO3 | 1.86E-11*exp( 175./t) |
| MACR + O3 → .8*CH3COCHO + .275*HO2 + .2*CO + .2*O3 + .7*CH2O + .215*OH | 4.40E-15*exp( -2500./t) |
| MACRO2 + NO → NO2 + .47*HO2 + .25*CH2O + .53*GLYALD + .25*CH3COCHO + .53*CH3CO3 + .22*HYAC + .22*CO | 2.70E-12*exp( 360./t) |
| MACRO2 + NO → 0.8*ONITR | 1.30E-13*exp( 360./t) |
| MACRO2 + NO3 → NO2 + .47*HO2 + .25*CH2O + .25*CH3COCHO + .22*CO + .53*GLYALD + .22*HYAC + .53*CH3CO3 | 2.40E-12 |
| MACRO2 + HO2 → MACROOH | 8.00E-13*exp( 700./t) |
| MACRO2 + CH3O2 → .73*HO2 + .88*CH2O + .11*CO + .24*CH3COCHO + .26*GLYALD + .26*CH3CO3 + .25*CH3OH + .23*HYAC | 5.00E-13*exp( 400./t) |
| MACRO2 + CH3CO3 → .25*CH3COCHO + CH3O2 + .22*CO + .47*HO2 + .53*GLYALD + .22*HYAC + .25*CH2O + .53*CH3CO3 | 1.40E-11 |
| MACROOH + OH → .5*MCO3 + .2*MACRO2 + .1*OH + .2*HO2 | 2.30E-11*exp( 200./t) |
| MCO3 + NO → NO2 + CH2O + CH3CO3 | 5.30E-12*exp( 360./t) |
| MCO3 + NO3 → NO2 + CH2O + CH3CO3 | 5.00E-12 |
| MCO3 + HO2 → .25*O3 + .25*CH3COOH + .75*CH3COOOH + .75*O2 | 4.30E-13*exp( 1040./t) |
| MCO3 + CH3O2 → 2*CH2O + HO2 + CO2 + CH3CO3 | 2.00E-12*exp( 500./t) |
| MCO3 + CH3CO3 → 2*CO2 + CH3O2 + CH2O + CH3CO3 | 4.60E-12*exp( 530./t) |
| MCO3 + MCO3 → 2*CO2 + 2*CH2O + 2*CH3CO3 | 2.30E-12*exp( 530./t) |
| MCO3 + NO2 + M → MPAN + M | 1.1E-11*300./t/[M] |
| MPAN + M → MCO3 + NO2 + M | k(MCO3 + NO2 + M) * 1.111E28 * exp(-14000/t) |
| MPAN + OH + M → .5*HYAC + .5*NO3 + .5*CH2O + .5*HO2 + 0.5*CO2 + M | ko=8.00E-27*(300/t)**3.50<br>ki=3.00E-11<br>f=0.50 |

**Table A2.** continued

| C-5 Degradation | |
|---|---|
| ISOP + OH → ISOPO2 | 2.54E-11*exp( 410./t) |
| ISOP + O3 → .4*MACR + .2*MVK + .07*C3H6 + .27*OH + .06*HO2 + .6*CH2O + .3*CO + .1*O3 + .2*MCO3 + .2*CH3COOH | 1.05E-14*exp( -2000./t) |
| ISOP + NO3 → ISOPNO3 | 3.03E-12*exp( -446./t) |
| ISOPO2 + NO → .08*ONITR + .92*NO2 + .23*MACR + .32*MVK + .33*HYDRALD + .02*GLYOXAL + .02*GLYALD + .02*CH3COCHO + .02*HYAC + .55*CH2O + .92*HO2 | 4.40E-12*exp( 180./t) |
| ISOPO2 + NO3 → HO2 + NO2 + .6*CH2O + .25*MACR + .35*MVK + .4*HYDRALD | 2.40E-12 |
| ISOPO2 + HO2 → ISOPOOH | 8.00E-13*exp( 700./t) |
| ISOPOOH + OH → .8*XO2 + .2*ISOPO2 | 1.52E-11*exp( 200./t) |
| ISOPO2 + CH3O2 → .25*CH3OH + HO2 + 1.2*CH2O + .19*MACR + .26*MVK + .3*HYDRALD | 5.00E-13*exp( 400./t) |
| ISOPO2 + CH3CO3 → CH3O2 + HO2 + .6*CH2O + .25*MACR + .35*MVK + .4*HYDRALD | 1.40E-11 |
| ISOPNO3 + NO → 1.206*NO2 + .794*HO2 + .072*CH2O + .167*MACR + .039*MVK + .794*ONITR | 2.70E-12*exp( 360./t) |
| ISOPNO3 + NO3 → 1.206*NO2 + .072*CH2O + .167*MACR + .039*MVK + .794*ONITR + .794*HO2 | 2.40E-12 |
| ISOPNO3 + HO2 → .206*NO2 + .206*CH2O + .206*OH + .167*MACR + .039*MVK + .794*ONITR | 8.00E-13*exp( 700./t) |
| BIGALK + OH → ALKO2 | 3.50E-12 |
| ONITR + OH → HYDRALD + .4*NO2 + HO2 | 4.50E-11 |
| ONITR + NO3 → HO2 + NO2 + HYDRALD | 1.40E-12*exp( -1860./t) |
| HYDRALD + OH → XO2 | 1.86E-11*exp( 175./t) |
| ALKO2 + NO → .4*CH3CHO + .1*CH2O + .25*CH3COCH3 + .9*HO2 + .8*MEK + .9*NO2 + .1*ONIT | 4.20E-12*exp( 180./t) |
| ALKO2 + HO2 → ALKOOH | 7.50E-13*exp( 700./t) |
| ALKOOH + OH → ALKO2 | 3.80E-12*exp( 200./t) |
| XO2 + NO → NO2 + HO2 + .25*CO + .25*CH2O + .25*GLYOXAL + .25*CH3COCHO + .25*HYAC + .25*GLYALD | 2.70E-12*exp( 360./t) |
| XO2 + NO3 → NO2 + HO2 + 0.5*CO + .25*HYAC + 0.25*GLYOXAL + .25*CH3COCHO + .25*GLYALD | 2.40E-12 |
| XO2 + HO2 → XOOH | 8.00E-13*exp( 700./t) |
| XO2 + CH3O2 → .3*CH3OH + .8*HO2 + .8*CH2O + .2*CO + .1*GLYOXAL + .1*CH3COCHO + .1*HYAC + .1*GLYALD | 5.00E-13*exp( 400./t) |
| XO2 + CH3CO3 → .25*CO + .25*CH2O + .25*GLYOXAL + CH3O2 + HO2 + .25*CH3COCHO + .25*HYAC + .25*GLYALD + CO2 | 1.30E-12*exp( 640./t) |
| XOOH + OH → H2O + XO2 | 1.90E-12*exp( 190./t) |
| XOOH + OH → H2O + OH | T**2 * 7.69E-17 * exp(253./t) |

**Table A2.** continued

| C-7 Degradation | Rate |
|---|---|
| TOLUENE + OH → .25*CRESOL + .25*HO2 + .7*TOLO2 | 1.70E-12*exp( 352./t) |
| TOLO2 + NO → .45*GLYOXAL + .45*CH3COCHO + .9*BIGALD + .9*NO2 + .9*HO2 | 4.20E-12*exp( 180./t) |
| TOLO2 + HO2 → TOLOOH | 7.50E-13*exp( 700./t) |
| TOLOOH + OH → TOLO2 | 3.80E-12*exp( 200./t) |
| CRESOL + OH → XOH | 3.00E-12 |
| XOH + NO2 → .7*NO2 + .7*BIGALD + .7*HO2 | 1.00E-11 |
| BENZENE + OH → BENO2 | 2.30E-12*exp( -193./t) |
| BENO2 + HO2 → BENOOH | 1.40E-12*exp( 700./t) |
| BENO2 + NO → 0.9*GLYOXAL + 0.9*BIGALD + 0.9*NO2 + 0.9*HO2 | 2.60E-12*exp( 350./t) |
| XYLENE + OH → XYLO2 | 2.30E-11 |
| XYLO2 + HO2 → XYLOOH | 1.40E-12*exp( 700./t) |
| XYLO2 + NO → 0.62*BIGALD + 0.34*GLYOXAL + 0.54*CH3COCHO + 0.9*NO2 + 0.9*HO2 | 2.60E-12*exp( 350./t) |
| C-10 Degradation | |
| C10H16 + OH → TERPO2 | 1.20E-11*exp( 444./t) |
| C10H16 + O3 → .7*OH + MVK + MACR + HO2 | 1.00E-15*exp( -732./t) |
| C10H16 + NO3 → TERPO2 + NO2 | 1.20E-12*exp( 490./t) |
| TERPO2 + NO → .1*CH3COCH3 + HO2 + MVK + MACR + NO2 | 4.20E-12*exp( 180./t) |
| TERPO2 + HO2 → TERPOOH | 7.50E-13*exp( 700./t) |
| TERPOOH + OH → TERPO2 | 3.80E-12*exp( 200./t) |
| Tropospheric Heterogeneous Reactions | |
| N2O5 → 2*HNO3 | |
| NO3 → HNO3 | |
| NO2 → 0.5*OH + 0.5*NO + 0.5*HNO3 | |
| CB1 → CB2 | 7.10E-06 |
| SO2 + OH → SO4 | |
| DMS + OH → SO2 | 9.60E-12*exp( -234./t) |
| DMS + OH → .5*SO2 + .5*HO2 | |
| DMS + NO3 → SO2 + HNO3 | 1.90E-13*exp( 520./t) |
| NH3 + OH → H2O | 1.70E-12*exp( -710./t) |
| OC1 → OC2 | 7.10E-06 |
| HO2 → 0.5*H2O2 | |
| Stratospheric removal rates for BAM aerosols | |
| CB1 → (No products) | 6.34E-08 |
| CB2 → (No products) | 6.34E-08 |
| OC1 → (No products) | 6.34E-08 |
| OC2 → (No products) | 6.34E-08 |
| SO4 → (No products) | 6.34E-08 |

**Table A2.** continued

| Stratospheric removal rates for BAM aerosols | |
|---|---|
| SOAM → (No products) | 6.34E-08 |
| SOAI → (No products) | 6.34E-08 |
| SOAB → (No products) | 6.34E-08 |
| SOAT → (No products) | 6.34E-08 |
| SOAX → (No products) | 6.34E-08 |
| NH4 → (No products) | 6.34E-08 |
| NH4NO3 → (No products) | 6.34E-08 |
| SSLT01 → (No products) | 6.34E-08 |
| SSLT02 → (No products) | 6.34E-08 |
| SSLT03 → (No products) | 6.34E-08 |
| SSLT04 → (No products) | 6.34E-08 |
| DST01 → (No products) | 6.34E-08 |
| DST02 → (No products) | 6.34E-08 |
| DST03 → (No products) | 6.34E-08 |
| DST04 → (No products) | 6.34E-08 |
| SO2t → (No products) | 6.34E-08 |
| **Sulfate aerosol reactions** | |
| N2O5 → 2*HNO3 | f (sulfuric acid wt%) |
| CLONO2 → HOCL + HNO3 | f (T,P,HCl,H2O,r) |
| BRONO2 → HOBR + HNO3 | f (T,P,H2O,r) |
| CLONO2 + HCL → CL2 + HNO3 | f (T,P,HCl,H2O,r) |
| HOCL + HCL → CL2 + H2O | f (T,P,HCl,HOCl,H2O,r) |
| HOBR + HCL → BRCL + H2O | f (T,P,HCl,HOBr,H2O,r) |
| **Nitric acid Di-hydrate reactions** | |
| N2O5 → 2*HNO3 | $\gamma$ = 0.0004 |
| CLONO2 → HOCL + HNO3 | $\gamma$ =0.004 |
| CLONO2 + HCL → CL2 + HNO3 | $\gamma$ =0.2 |
| HOCL + HCL → CL2 + H2O | $\gamma$ =0.1 |
| BRONO2 → HOBR + HNO3 | $\gamma$ = 0.3 |
| **Ice aerosol reactions** | |
| N2O5 → 2*HNO3 | $\gamma$ = 0.02 |
| CLONO2 → HOCL + HNO3 | $\gamma$ =0.3 |
| BRONO2 → HOBR + HNO3 | $\gamma$ = 0.3 |
| CLONO2 + HCL → CL2 + HNO3 | $\gamma$ = 0.3 |
| HOCL + HCL → CL2 + H2O | $\gamma$ = 0.2 |
| HOBR + HCL → BRCL + H2O | $\gamma$ = 0.3 |
| **Synthetic tracer reactions** | |
| $NH_5$ → (No products) | 2.31E-06 |
| $NH_{50}$ → (No products) | 2.31E-07 |
| $NH_{50W}$ → (No products) | 2.31E-07 |
| $ST80_{25}$ → (No products) | 4.63E-07 |
| $CO_{25}$ → (No products) | 4.63E-07 |
| $CO_{50}$ → (No products) | 2.31E-07 |
| E90 → (No products) | 1.29E-07 |
| $E90_{NH}$ → (No products) | 1.29E-07 |
| $E90_{SH}$ → (No products) | 1.29E-07 |

**Table A3.** Tropospheric ozone production and loss rates calculated for explict reaction rates, O3-Prod and O3-Loss are the sum of the specific reaction rates.

| Production / Loss (Tg/yr) | REFC1SD | REFC1 | REFC2 |
|---|---|---|---|
| O3-Prod | 4701.1 | 4716.5 | 4758.0 |
| NO-HO2 | 3032.2 | 3017.3 | 3051.7 |
| CH3O2-NO | 1102.1 | 1078.6 | 1072.2 |
| PO2-NO | 19.8 | 20.9 | 21.1 |
| CH3CO3-NO | 159.6 | 168.8 | 172.3 |
| C2H5O2-NO | 8.2 | 8.1 | 7.5 |
| 0.92*ISOPO2-NO | 113.0 | 131.8 | 136.1 |
| MACRO2-NOa | 60.9 | 68.3 | 69.9 |
| MCO3-NO | 25.6 | 28.9 | 29.8 |
| C3H7O2-NO | n.a. | n.a. | n.a. |
| RO2-NO | 10.6 | 11.2 | 11.6 |
| XO2-NO | 53.6 | 62.4 | 64.1 |
| 0.9*TOLO2-NO | 2.7 | 2.8 | 3.8 |
| TERPO2-NO | 15.2 | 16.7 | 16.8 |
| 0.9*ALKO2-NO | 21.6 | 21.3 | 21.7 |
| ENEO2-NO | 12.0 | 12.4 | 12.5 |
| EO2-NO | 34.9 | 37.2 | 37.0 |
| MEKO2-NO | 16.4 | 16.1 | 16.7 |
| 0.4*ONITR-OH | 6.0 | 6.8 | 7.1 |
| jonitr | 1.1 | 1.2 | 1.3 |
| O3-Loss | 4118.0 | 4128.9 | 4157.6 |
| O1D-H2O | 2217.8 | 2295.8 | 2290.2 |
| OH-O3 | 582.2 | 537.6 | 536.7 |
| HO2-O3 | 1203.5 | 1179.0 | 1202.4 |
| C3H6-O3 | 11.9 | 11.0 | 12.0 |
| 0.9*ISOP-O3 | 51.3 | 51.9 | 59.4 |
| C2H4-O3 | 7.9 | 8.0 | 8.1 |
| 0.8*MVK-O3 | 12.9 | 13.5 | 14.8 |
| 0.8*MACR-O3 | 2.4 | 2.4 | 2.7 |
| C10H16-O3 | 28.2 | 29.6 | 31.4 |